

## University of Groningen

### Positron emission tomography (PET) in head and neck oncology.

Braams, Jan Willem

**IMPORTANT NOTE: You are advised to consult the publisher's version (publisher's PDF) if you wish to cite from it. Please check the document version below.**

*Document Version*

Publisher's PDF, also known as Version of record

*Publication date:*

1998

[Link to publication in University of Groningen/UMCG research database](#)

*Citation for published version (APA):*

Braams, J. W. (1998). *Positron emission tomography (PET) in head and neck oncology*. [Thesis fully internal (DIV), University of Groningen]. [S.n.].

**Copyright**

Other than for strictly personal use, it is not permitted to download or to forward/distribute the text or part of it without the consent of the author(s) and/or copyright holder(s), unless the work is under an open content license (like Creative Commons).

The publication may also be distributed here under the terms of Article 25fa of the Dutch Copyright Act, indicated by the "Taverne" license. More information can be found on the University of Groningen website: <https://www.rug.nl/library/open-access/self-archiving-pure/taverne-amendment>.

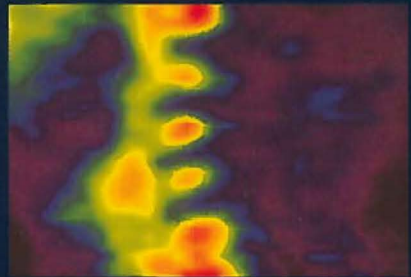
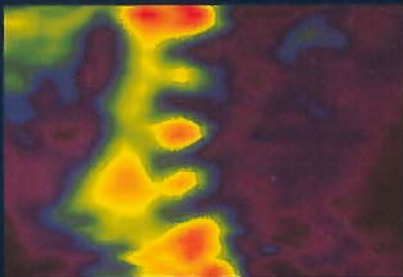
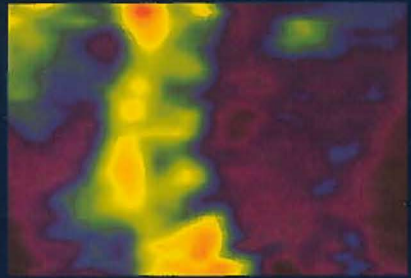
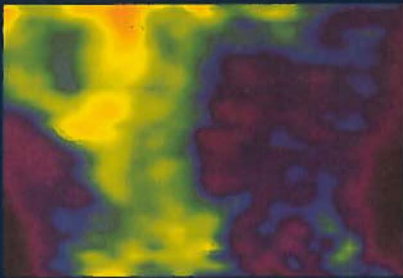
**Take-down policy**

If you believe that this document breaches copyright please contact us providing details, and we will remove access to the work immediately and investigate your claim.

Downloaded from the University of Groningen/UMCG research database (Pure): <http://www.rug.nl/research/portal>. For technical reasons the number of authors shown on this cover page is limited to 10 maximum.

*Positron emission tomography (PET)  
in head and neck oncology*

*Jan Willem Braams*



*Positron emission tomography (PET)  
in head and neck oncology*



**STELLINGEN**  
BEHOREND BIJ HET PROEFSCHRIFT

**POSITRON EMISSION TOMOGRAPHY (PET)**  
**IN HEAD AND NECK ONCOLOGY**

1. Aan de waarde van PET-FDG bij patiënten met palpabele halsklieren bij een planocellulair carcinoom van de bovenste adem- en voedingsweg moet worden getwijfeld.  
(dit proefschrift)
2. Het begrip "metastase van een onbekende primaire tumor" is nog steeds actueel.  
(dit proefschrift)
3. De waarde van PET wordt kan verder worden vergroot door anatomische en functionele beeldvorming te combineren.  
(dit proefschrift)
4. PET onderzoek wordt door een cyclotron bepaald.  
(dit proefschrift)
5. In de huidige maatschappij staat kiezen op de voorgrond.
6. Een rigide interval voor de tandheelkundige controle wijst op gebrek aan inzicht in de mondgezondheid.
7. Gezien het feit dat tandsteen primair ontstaat op plaatsen waar niet wordt gepoetst, moet aan de effectiviteit van antitandsteen-tandpasta worden getwijfeld.
8. Bij de opname in een nationale sportselectie zou het overleggen van een bewijs van goed gedrag verplicht moeten zijn.
9. Versterven in doodgewoon
10. In van Dale's woordenboek der Nederlandse taal dient het woord "gumusen" te worden opgenomen met de bijbehorende verklaring: het van overheidswege uitsluitend op legalistische gronden terugsturen van een persoon, of een uit meerder personen bestaande familieeenheid naar het land van herkomst, ondanks dat er een onafhankelijk bestaan is opgebouwd en aan de maatschappelijke verplichtingen wordt voldaan.
11. Alle sport is topsport als er sprake is van een maximale prestatie.
12. De voordelen tengevolge van de 24-uurs economie veranderende arbeidsvoorwaarden worden zowel door werkgevers als werknemers onderbelicht.
13. Vrouwen die verkiezen geen baan te hebben maar voor het thuisfront te zorgen tonen in de huidige maatschappij meer karakter dan diegenen die ondanks alles willen werken.



*Rijksuniversiteit Groningen*

*Positron emission tomography (PET)  
in head and neck oncology*

*Proefschrift*

*Ter verkrijging van het doctoraat in de Medische Wetenschappen  
aan de Rijksuniversiteit Groningen  
op gezag van de Rector Magnificus, dr. D.F.J. Bosscher  
in het openbaar te verdedigen op  
woensdag 30 september 1998  
om 16.15 uur  
door*

*Jan Willem Braams*

*geboren 20 november 1965  
te Enschede*

*Promotores:*        *Prof.Dr. J.L.N. Roodenburg*  
                          *Prof.Dr. W. Vaalburg*  
                          *Prof.Dr. A. Vermey*

*Referenten:*        *Dr. P.G.J. Nikkels*  
                          *Dr. J. Pruim*

*ISBN 90-367-0894-x*



*voor Annet  
&  
mijn ouders*

*Promotiecommissie:*      *Prof. Dr. W.M. Molenaar*  
                                      *Prof. Dr. F.W.J. Albers*  
                                      *Prof. Dr. S.N. Reske*

*Paranimfen:*                *Dr. M.J.H. Witjes*  
                                      *F.A.B. Woldring*

*Contribution to the printing costs of this thesis was made by:*  
*Knoll bv*

*Drukwerk: Grafisch Bedrijf Ponsen & Looijen BV, Wageningen*

# CONTENTS

		page
CHAPTER 1	<b>Introduction and aim of the study</b>	1
CHAPTER 2	<b>Assessment of lymph nodes in the neck area</b>	9
	2.1 Introduction	
	2.2 Topographic anatomy	
	2.3 Classification of metastatic lymph nodes	
	2.4 Pattern of lymphatic spread of head and neck squamous cell carcinoma	
	2.5 Assessment of lymph nodes	
	2.6 Definition of quantitative parameters	
CHAPTER 3	<b>Detection of lymph node metastases of squamous cell cancer of the head and neck with FDG-PET and MRI</b>	21
	3.1 Introduction	
	3.2 Materials and Methods	
	3.3 Results	
	3.4 Discussion	
CHAPTER 4	<b>Nodal spread of squamous cell carcinoma of the oral cavity detected with PET-tyrosine, MRI and CT</b>	39
	4.1 Introduction	
	4.2 Materials and Methods	
	4.3 Results	
	4.4 Discussion	
CHAPTER 5	<b>Detection of metastatic lymph nodes in the head and neck area with PET-tyrosine in whole body mode</b>	53
	5.1 Introduction	
	5.2 Materials and Methods	
	5.3 Results	
	5.4 Discussion	

<b>CHAPTER 6</b>	<b>Detection of oral dysplasia in animals with FDG and Tyrosine</b>	<b>65</b>
	6.1 Introduction	
	6.2 Materials and Methods	
	6.3 Results	
	6.4 Discussion	
<b>CHAPTER 7</b>	<b>Detection of unknown primary head and neck tumors with the use of Positron Emission Tomography</b>	<b>79</b>
	7.1 Introduction	
	7.2 Materials and Methods	
	7.3 Results	
	7.4 Discussion	
<b>CHAPTER 8</b>	<b>Summary and General Discussion</b>	<b>89</b>
	8.1 Introduction	
	8.2 The assessment of metastatic lymph nodes	
	8.3 In vivo measurements of dysplasia	
	8.4 Unknown primary tumors	
	8.5 General discussion	
	<b>Samenvatting</b>	<b>97</b>
Curriculum Vitae		
Dankwoord		

- CHAPTER 1 -

INTRODUCTION  
AND  
AIM OF THE STUDY

In the last 25 years, Positron Emission Tomography (PET) has been developed in basic research and is now available for clinical, physiological and pathophysiological research and for diagnosis. PET is based on the administration of tracers labeled with short-lived positron emitting radionuclides as e.g.  $^{11}\text{C}$  ( $t_{1/2}=20$  min.),  $^{13}\text{N}$  ( $t_{1/2}=10$  min.),  $^{15}\text{O}$  ( $t_{1/2}=2$  min.) and  $^{18}\text{F}$  ( $t_{1/2}=110$  min.). These radionuclides are generated by bombardment of appropriate target materials with cyclotron-accelerated charged particles, e.g. protons. After the separation from the target material, these radionuclides produced are incorporated into organic compounds by means of a radiochemical synthesis. These organic compounds are designed to become incorporated in specific biochemical processes. After purification and sterilization, the radiolabeled compounds are used as radiochemical tracers (radiopharmaceuticals). When injected intravenously into a biological organism, the radiopharmaceutical distributes into the tissues and especially in those tissues with biochemical processes in which the organic compound is specifically needed. In the tissue, positron-electron annihilation produces two 511 keV gamma-rays, which are detected by a camera, externally positioned to the body. From the acquired data, computerized images are generated, representing the quantitative spatial distribution of the radioactivity in the body. The software of the computer allows for image reconstruction in every desirable plane. The distribution of radioactivity can be obtained in time. Since quantitative parameters of biochemical processes (e.g. protein synthesis rates, DNA synthesis rates, glycolysis) are desired, the dynamic PET data are implemented into mathematical models that describe the kinetics of the radiopharmaceutical and its labeled metabolites in the tissue. From these mathematical models, rates of specific biochemical processes are calculated (1).

So, in contrast to ultrasound (US), magnetic resonance imaging (MRI) or computed tomography (CT), PET offers information on metabolic processes. The mentioned imaging modalities offer primarily structural information while PET yields mainly biochemical information. PET is very useful to investigate and image metabolic parameters of tumor tissue (in vivo).

This alternative way of cancer imaging is used to study the physicochemical properties of tumor cells. It is expected that alterations in metabolism precede structural alterations and that registration of these alterations may improve the detection of cancer. A high rate of glycolysis is the biochemical hallmark of many types of tumor cells (2). The transition from slowly growing and well-differentiated to rapidly growing and poorly

differentiated neoplasms is very often reflected by progressive increase in anaerobic glycolysis and protein synthesis rates. The increased glycolysis can be monitored with PET, using the glucose analogue 2-deoxy-2-[<sup>18</sup>F]fluoro-D-glucose (FDG) (3). The protein synthesis rate can be investigated with the use of amino acids as e.g. L-[1-<sup>11</sup>C]-tyrosine (TYR) (4-7). With these two tracers it is possible to utilise the biochemical properties of tumor cells for visualisation with PET. The detection possibilities of PET are determined by the properties of the radiopharmaceuticals and the resolution of the camera (4,8-10).

In head and neck oncology, squamous cell carcinomas (SCC's) of the upper aerodigestive tract are a heterogeneous group of tumors but they share a number of etiologic and biologic behavioral characteristics. These tumors develop in a relatively short time (months) and give rise to metastases in regional lymph nodes in the neck. It is well known that the presence and extent of lymph node metastases in the neck is one of the most important prognostic factors, not only in terms of loco-regional recurrence, but also in terms of distant metastases and survival (11,12). If metastatic lymph nodes are not present at the initial treatment but develop in the course of the disease, cure rates decrease. The overall prognosis decreases with 50% with the presence of lymph node metastases (13-24).

The assessment of clinically occult metastatic lymph nodes from primary tumors of SCC is very difficult. However, there is clinical relevance in detecting such occult metastases since the treatment is determined by the presence or absence of metastatic lymph nodes.

Imaging techniques such as US, MRI and CT have improved the staging of the neck as compared to palpation. These imaging modalities monitor tumors or lymph node metastases by size and structural changes. However, this assessment remains limited (11,12). The CT and MRI determination of lymph node involvement is mainly based upon nodal size. The size criterium decreases the accuracy because inflammatory nodes may be enlarged and lymph node metastases may be normal in size. As a consequence, specificity of these techniques is increased at the cost of lowering the sensitivity, since smaller lymph nodes with no irregular enhancement are excluded by definition. Another important development in the assessment of the neck is the US guided fine needle aspiration cytology. This is an invasive technique and needs special skills of the operator.

However a high sensitivity and specificity can be reached (25).

Consequently, a non-invasive imaging modality that can detect lymph node metastases with a higher sensitivity and higher specificity could be useful for accurate treatment planning of head and neck cancer. PET, reflecting changes in biological activity, may be such a valuable modality.

An intriguing problem in clinical oncology is the management of patients with a lymph node metastasis or metastases from an unknown primary tumor. In 5-10% of all cancer patients the site of the primary tumor is not known (25). Failure to detect the primary tumor site in patients with metastatic cancer in neck lymph nodes represents 2-3% of the total head and neck cancer cases (26).

In cases of SCC lymph node metastases located in the upper two thirds of the neck the unknown primary tumor is most likely situated in the head and neck area. An accepted treatment consists of a radical or modified radical neck dissection followed by radiation therapy to both sides of the neck, including the mucosal surfaces of the entire upper aerodigestive tract in order to treat all possible tumor sites, such as nasopharynx, tonsils, base of tongue and pyriform sinuses. This treatment has a high morbidity rate consisting of severe xerostomia, mucosal atrophy and an increased risk for osteoradionecrosis of the jaw bones. To decrease the morbidity it would be of value to localize the primary tumor. A more purposeful treatment could then be given. In principle PET might be useful in the detection of these unknown primary tumors.

Because PET reflects differences in biological activity, it is theoretically possible that also premalignant lesions can be detected. To investigate premalignant lesions and cancer, animal models have been developed. Such models are useful to study the pathogenesis of these lesions and to evaluate diagnostic and therapeutic modalities.

Tumors in animals can be created by induction with a carcinogen or by transplantation of tumor cells into an animal. The advantage of an animal model with an induced tumor compared to a model with a transplanted tumor is the presence of a premalignant stage. These chemically induced tumors and premalignant stages are comparable with human lesions (27,28). A disadvantage of inducing tumors is that it is a time consuming method that needs 2 or 3 weekly applications for several weeks to months.



The insight in the biological behaviour and better staging possibilities can lead to modified and less mutilating procedures for head and neck cancer. PET is a new diagnostic approach in this field and the value of PET in the management of head and neck cancer should be widely explored.

*Aim of the study*

The development of PET to monitor protein synthesis rate and glucose metabolism in tumors has provided opportunities to answer questions which are of significant importance in head and neck oncology. The general aim of the work presented in this thesis was to investigate the potential of PET in combination with FDG and TYR as radiopharmaceuticals in the treatment planning of patients with SCC of the oral cavity.

*Chapter 3.* The aim of this study was to investigate the value of FDG-PET in the identification of cervical lymph node metastases of SCC of the oral cavity and oropharynx, compared to analysis of clinical, MRI and histopathologic findings.

*Chapter 4.* The aim of this study was to investigate whether cervical metastatic spread of SCC of the oral cavity can be visualized with TYR-PET and to compare these results with the clinical, MRI, CT and histopathologic findings. Also a comparison was made with the data described in chapter 3 from the group of patients studied with FDG.

*Chapter 5.* PET-imaging, as applied in the previous chapters, is inconvenient for the patient. It is time consuming and requires the patient to lie still for a long time (2 hrs). The aim of this study was to investigate whether the whole body scanning technique for the head and neck region, which takes less camera time (30 minutes), yields similar results as those in our previous studies.

*Chapter 6.* The aim of this study was to investigate the value of PET with the two tracers FDG and TYR in detecting the premalignant stages and SCC induced by 4-nitroquinoline 1-oxide (4NQO) in the palatal mucosa of a male Whistar albino rat as a function of time of application of this carcinogen.

*Chapter 7.* The aim of this study was to investigate the potential value of FDG-PET for the detection of unknown primary tumors in patients with cervical lymph node metastases.

---

**References**

- 1 Conti PS, Lilien DL, Hawley K, et al. PET and [<sup>18</sup>F]-FDG in oncology: A clinical update. *Nucl Med Biol* 1996;6:717-735.
- 2 Warburg O. The metabolism of tumors. London: Arnold Constable 1930;75-327.
- 3 Minn H, Joensuu H, Ahonen A, Klemi P. Fluorodeoxyglucose imaging: a method to assess the proliferative activity of human cancer in vivo. *Cancer* 1988;61:1776-1781.
- 4 Ishiwata K, Kubota K, Murakami M. et al. Re-evaluation of amino acid-pet studies: can the protein synthesis rates in the brain and tumor tissues be measured in vivo ? *J Nucl Med* 1993;34: 1936-1943.
- 5 Daemen BJG, Elsinga PH, Paans AMJ, Wieringa AR, Konings AWT, Vaalburg W. Radiation-induced inhibition of tumor growth as monitored by PET using L-1-[<sup>11</sup>C]-tyrosine and <sup>18</sup>F-fluoride-oxyglucose. *J Nucl Med* 1992;33:373-379.
- 6 Daemen BJG, Zwertbroek R, Elsinga PH, Paans AMJ, Doorenbos H, Vaalburg W. PET studies with L-1-[<sup>11</sup>C]-tyrosine, L-[methyl-<sup>11</sup>C]methionine and 18FDG in prolactinomas in relation to bromocryptine treatment. *Eur J Nucl Med* 1991;18:453-460.
- 7 Willemsen ATM, van Waarden A, Paans AMJ, et al. In vivo protein synthesis rate determination in primary or recurrent brain tumors using L-[1-<sup>11</sup>C]-Tyrosine and PET. *J Nucl Med* 1995;36: 411-419.
8. Tahara T, Ichiya Y, Kuwabara Y, et al. High [<sup>18</sup>F]fluorodeoxyglucose uptake in abdominal abscesses: a PET study. *J Comput Assist Tomogr* 1989;13:829-831.
9. Sasaki M, Ichiya Y, Kuwabara Y, et al. Ringlike uptake of [<sup>18</sup>F]FDG in brain abscess: a PET study. *J Comput Assist Tomogr* 1990;14:486-487.
10. Kubota R, Yamada S, Kubota K, Ishiwata K, Tamahashi N, Ido T. Intratumoral distribution of fluorine-18-fluorodeoxyglucose in vivo: High accumulation in macrophages and granulation tissues studied by microautoradiography. *J Nucl Med* 1992;33:1972-1980.
11. Van den Brekel MWM, Castelijns JA, Croll GA, et al. Magnetic resonance imaging versus palpation of cervical lymph node metastases. *Arch Otolaryngol Head Neck Surg* 1991;117:666-673.
12. Van den Brekel MWM, Stel HV, Castelijns JA, et al. Cervical lymph node metastasis: assesment of radiologic criteria. *Radiology* 1990;177:379-384.
- 13 Spiro RH, Alfonso AE, Farr HW, Strong EW. Cervical node metastasis from epidermoid carcinoma of the oral cavity and oropharynx. A critical assesment of current staging. *Am J Surg* 1974;128:562-567.
- 14 Snow GB, Annyas AA, van Slooten EA, Bartelink H, Hart AAM. Prognostic factors of neck node metastasis. *Clin Otolaryngol* 1982;7:185-192.
- 15 Kalnins IK, Leonard AG, Sako K, Razack MS, Shedd DP. Correlation between prognosis and degree of lymph node involvement in carcinoma of the oral cavity. *Am J Surg* 1977;134:450-

454.

- 16 Noone RB, Bonner H, Raymond S, Brown AS, Graham WP, Lehr HB. Lymph node metastasis in oral carcinoma. A correlation of histopathology with survival. *Plast Reconstr Surg* 1974;53: 158-166.
- 17 Shah JP, Cendon RA, Farr HW, Strong EW. Carcinoma of the oral cavity. Factors affecting treatment failure at the primary site and neck. *Am J Surg* 1976;132:504-507.
- 18 Cachin Y, Sancho-Garnier H, Micheau C, Marandas P. Nodal metastasis from carcinoma of the oropharynx. *Otolaryngol Clin N Am* 1979;12: 145-154.
- 19 Shah JP. Cervical lymph node metastases - diagnostic, therapeutic, and prognostic implications. *Oncology* 1990;4:61-69.
- 20 Lefebvre JL, Castelain B, De La Torre JC, Delobelle-Deroide A, Vankemmel B. Lymph node invasion in hypopharynx and lateral epilynx carcinoma: a prognostic factor. *Head Neck Surg* 1987;10:14-18.
- 21 Ditroia JF. Nodal metastasis and prognosis in carcinoma of the oral cavity. *Otolaryngol Clin N Am* 1972;5:333-342.
- 22 Schuller DE, McGuirt WF, McCabe BF, Young D. The prognostic significance of metastatic cervical lymph nodes. *Laryngoscope* 1980;90:557-570.
- 23 Ganzer U, Meyer-Breiting E, Ebberts J, Vosteen KH. Der Einfluß von Tumorgroße, Lymphknotenbefall und Behandlungsart auf Prognose des Hypopharynxkarzinoms. *Laryng Rhinol Otol* 1982;61:622-628.
- 24 Leemans CR, Tiwari RM, van der Waal I, Karim ABMF, Nauta JJP, Snow GB. The efficacy of comprehensive neck dissection with or without postoperative radiotherapy in nodal metastases of squamous cell carcinoma of the upper respiratory and digestive tracts. *Laryngoscope* 1990;100: 1194-1198.
- 25 Van den Brekel MWM, Castelijns JA, Stel HV, et al. Modern imaging techniques and ultrasound-guided aspiration cytology for the assessment of neck node metastases: a prospective comparative study. *Eur Arch Otorhinolaryngol* 1993;250:11-17.
- 26 Million RR, Cassisi NJ, eds. Management of head and neck cancer. A multidisciplinary approach. 2nd edition. Philadelphia: J.B. Lippencott Co. 1994;311-320.
- 27 Nauta JM, Roodenburg JLN, Nikkels PGJ, Witjes MJH, Vermey A. Comparison of epithelial dysplasia. The 4NQO rat palatal model versus human oral mucosa. *Int J Oral Maxillofac Surg* 1995;24:53-58.
- 28 Prime SS, Malamos D, Rosser TJ, Scully CM. Oral epithelial atypia and acantholytic dyskeratosis in rats painted with 4-nitroquinoline N-oxide. *J Oral Pathol* 1986;15:280-283.

- CHAPTER 2 -

ASSESSMENT OF  
LYMPH NODES IN THE NECK AREA

## 2.1 Introduction

Squamous cell carcinomas of the mucosal surfaces of the upper aerodigestive tract have a tendency to spread to regional lymph nodes in the neck. This can happen already in an early stage of the disease. Since the extent and type of treatment is not only determined by the size and location of the primary tumor but also by the presence or absence of metastatic lymph nodes, the assessment of these nodes is of great significance. Imaging modalities play an important role in the detection of non-palpable metastatic lymph nodes, the so called "subclinical disease" (1).

This chapter gives an overview of the topographic anatomy (2) and the classification of cervical lymph nodes (3-5). Furthermore, the assessment of lymph node metastases with several imaging modalities and the diagnostic process will be discussed. To compare the different imaging modalities with each other statistical analysis will be used. This will be explained in the last paragraph of this chapter (2.6).

## 2.2 Topographic anatomy

The topographical classification of cervical lymph nodes is complicated because of the several different systems that are used. The specific names for particular nodes are loosely intermixed between one classification system and another. Considering head and neck cancer, the clinically most important lymph nodes are the submental, submandibular (or submaxillary) and the lateral cervical groups (fig 1).

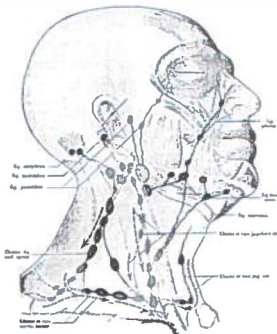


**Figure 1.** Lymph node groups according to Rouvière (2).

2.2.1. The submental group is situated in the submental triangle of the neck, caudally to the mylohyoid muscle and between the anterior bellies of the digastric muscles, the hyoid bone and the lower border of the mandibular symphysis. The one to eight lymph nodes in this group drain the chin, lower lip, anterior lower gingiva, floor of the mouth, and tip of the tongue. From here lymph drains into the submandibular nodes and internal jugular chain (of the lateral cervical nodes).

2.2.2. The submandibular (or submaxillary) group consists of three to twelve nodes and is situated below the mylohyoid muscle in the triangle bounded by the two bellies of the digastric muscle and the lower border of the mandible. These nodes drain the lateral portion of the chin, the lower and upper lips, cheek, skin of the nose, anterior nasal fossae, most of the gums, teeth, palate, anterior portion of the tongue, medial portion of the eyelids, submandibular and sublingual glands, and the floor of the mouth. The filtered lymph drains into the internal jugular chain (of the lateral cervical nodes).

2.2.3. The anterior cervical group of nodes in the infrahyoid portion of the neck, between the two carotid sheaths, consists of two divisions: the anterior jugular chain and the juxta-visceral group. The anterior (superficial) jugular chain follows the course of the anterior jugular vein and is situated in the superficial fascia of the neck, overlying the strap muscles. These one to four small, inconstant nodes drain the skin and muscles of the anterior portion of the neck, and their lymph drains into the thoracic duct or anterior mediastinal nodes on the left side and into the lowest internal jugular chain or highest intrathoracic node on the right side. The juxta-visceral group is situated along the larynx, the trachea, the thyroid and the recurrent laryngeal nerves.

2.2.4. The internal jugular chain lies along the internal jugular vein. The fifteen to forty nodes in the deep cervical chain are situated between the level of the crossing of the posterior belly of the digastric muscle and the internal jugular vein (subdigastric nodes) cranially and the level where the internal jugular vein ends into the brachiocephalic vein caudally. The omohyoid muscle divides the jugular chain into two clinically relevant groups: the supra-omohyoid group and the infra-omohyoid group. The supra-omohyoid (superior jugular) group of nodes is situated anterolateral to the vein. The infra-omohyoid (inferior jugular) nodes lie anterior, medial, or posterior to the vein. These cervical

nodes drain the parotid, submandibular, submental, retropharyngeal, and some anterior cervical nodes.

2.2.5. The spinal accessory chain of nodes follows the course of the spinal accessory nerve in the posterior triangle of the neck. There are four to twenty nodes in this group. These nodes drain the occipital and mastoid nodes, the parietal and occipital regions of the scalp, the nape and lateral portions of the neck, and the upper part of the shoulder. Their lymph drains primarily into the transverse cervical chain, and from there into the lower part of the internal jugular chain.

2.2.6. The transversal cervical nodes follow the course of the transverse cervical vessels. The one to ten nodes in this group primarily connect the accessory chain and the inferior jugular nodes: on the left, the ductus thoracicus and on the right the truncus lymphaticus dexter. The transverse cervical nodes also receive lymph from the anterolateral portion of the neck, and the upper anterior chest wall.

2.2.7. The upper occipital nodes are located at the junction of the upper posterior portion of the neck and the lower lateral cranial vault. There are three to ten nodes in this group; draining the occipital region and flowing primarily into the spinal accessory chain of the lateral cervical nodes.

2.2.8. The lower occipital nodes form a small group of one to three nodes. These are located under the origin of the trapezius muscle tendon and extend downward and parallel to the midline.

2.2.9. The retropharyngeal nodes are divided in a median and a lateral group. The medial group is found near the midline, usually located directly posterior to the upper pharynx near the level of the second cervical vertebra. This group consists of no more than one or two nodes. The lateral group contains one to three nodes, and is situated near the lateral aspect of the posterior pharyngeal wall, overlying the longus capitis and longus colli muscles. The retropharyngeal nodes are located medially to the carotid artery. The whole retropharyngeal group primarily drains the posterior nasopharynx and oropharynx, but drains also the soft palate and paranasal sinuses. Their lymph ultimately



drains into the superior internal jugular chain of the lateral cervical nodes.

2.2.10. The parotid nodes are situated around the parotid gland and within the glandular tissue and count for seven to nineteen nodes. These nodes drain an extensive and varied territory, including the forehead and temporal regions, portions of the midface and lateral parts of the face, the lateral auricle and external auditory canal, the eustachian tube, portions of the posterior part of the cheek (buccal mucous membrane), and the parotid gland. The lymph from these nodes flows through a variety of local pathways to the internal jugular chain of the lateral cervical nodes.

2.2.11. The buccal facial nodes are found in the subcutaneous tissues of the cheek and, in general, follow the course of the (external) facial artery and the anterior facial vein. This group consists of five to ten nodes draining the eyelids, cheek, mid portion of the face, and the gums and palate. The facial nodes drain into the submandibular nodes.

2.2.12. The retroauricular nodes are situated behind the auricle. There are one to four nodes that drain the parotid region, parietal area, and skin of the posterior auricle. Their lymph flows into the inferior parotid nodes and superior internal jugular chain of the lateral cervical nodes.

### **2.3 Classification of metastatic lymph nodes**

The assessment of the neck is still mainly based upon palpation. Palpable lymph nodes are classified according to size, consistency and localisation. Originally there were two major TNM (tumor, node, metastases) classifications: the first was developed by the International Union Against Cancer (UICC)(3), the second was designed by the American Joint Committee on Cancer (AJCC)(4). Since 1987 these staging classifications are the same.

The N-categories are now based on physical examination and imaging. The accuracy of palpation with regard to number and size of involved nodes leaves much to be desired.

Stage	Characteristics
NX	Regional lymph nodes cannot be assessed
N0	No regional lymph node metastasis
N1	Metastasis in a single ipsilateral lymph node, 3 cm or less in greatest dimension
N2	Metastasis in a single ipsilateral lymph node, more than 3 cm but not more than 6 cm in greatest dimension; <i>or</i> in multiple ipsilateral lymph nodes, none more than 6 cm in greatest dimension; <i>or</i> in bilateral or contralateral lymph nodes, none more than 6 cm in greatest dimension
N2a	Metastasis in a single ipsilateral lymph node, more than 3 cm but not more than 6 cm in greatest dimension
N2b	Metastasis in multiple ipsilateral lymph nodes, none more than 6 cm in greatest dimension
N2c	Metastasis in bilateral or contralateral lymph nodes, none more than 6 cm in greatest dimension
N3	Metastasis in a lymph node more than 6 cm in greatest dimension

**Figure 2.** Staging of metastatic lymph nodes in the neck (3).

### 2.4 Patterns of lymphatic spread

Although many different pathways of lymphatics in the neck exist, most metastases from primary tumors in the head and neck area follow a rather constant route via local lymph nodes to lymph nodes more deep in the neck. The knowledge of these patterns is very important for the clinical management. To eliminate potential misinterpretation, overlap and lack of standardization, a nomenclature system was developed. This framework provides a system on which subsequent terminology can be added. In this framework the neck is divided in 6 levels (5).

- Level I:** Submental group - Lymph nodes within the the triangular boundary of the anterior belly of the digastric muscles and the hyoid bone.  
Submandibular group - Lymph nodes within the boundaries of the anterior and posterior bellies of the digastric muscle and the body of the mandible. The submandibular gland is included in the specimen when the lymph nodes within this triangle are removed.
- Level II:** Upper jugular group - Lymph nodes located around the upper third of the internal jugular vein and adjacent spinal accessory nerve extending from the level of the carotid bifurcation (surgical landmark) or hyoid bone (clinical landmark) to the skull base. The posterior boundary is the posterior border of the sternocleido mastoid muscle and the anterior boundary is the lateral border of the stylohyoid muscle.
- Level III:** Middle jugular group - Lymph nodes located around the middle third of the internal jugular vein extending from the carotid bifurcation superiorly to the omohyoid muscle (surgical landmark), or cricothyroid notch (clinical landmark) inferiorly. The posterior boundary is the posterior border of the sternocleidomastoid muscle, and the anterior boundary is the lateral border of the sternohyoid muscle.
- Level IV:** Lower jugular group - Lymph nodes located around the lower third of the internal jugular vein extending from the omohyoid muscle superiorly to the clavicle inferiorly. The posterior boundary is the posterior border of the sternocleidomastoid muscle, and the anterior boundary is the lateral border of the sternohyoid muscle.
- Level V:** Posterior triangle group - This group comprises predominantly the lymph nodes located along the lower half of the spinal accessory nerve and the transverse cervical artery. The supraclavicular nodes are also included in this group. The posterior boundary is the anterior border of the trapezius muscle, the anterior boundary is the posterior border of the sternocleidomastoid muscle, and the inferior boundary is the clavicle.
- Level VI:** Anterior compartment group - This group comprises lymph nodes surrounding the midline visceral structures of the neck extending from the level of the hyoid bone superiorly to the suprasternal notch inferiorly. On each side, the lateral boundary is the medial border of the carotid sheath. Located

within this compartment are perithyroidal lymph nodes, paratracheal lymph nodes, lymph nodes along recurrent laryngeal nerves, and precricoid lymph nodes.

This staging framework is now generally accepted.

- Level I : the submental and submandibular group.
- Level II : the upper jugular group
- Level III: the middle jugular group
- Level IV: the lower jugular group
- Level V : the posterior triangle group
- Level VI: the anterior compartment group.

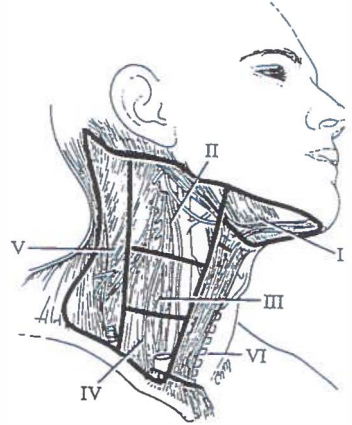


**Figure 3.** The level system for describing the location of lymph nodes in the neck (5).

### 2.5 Assessment of lymph nodes

Nowadays there are several modalities available for the assessment of the neck. Magnetic resonance imaging (MRI), computed tomography (CT), ultrasound (US) and US guided fine needle aspiration cytology (USgFNAC) are used for this purpose. These diagnostic modalities have improved tumor classification (T stage) and the staging of the neck as compared to palpation. With these techniques, it is possible to monitor tumors and metastases by size and structural changes or even to obtain cytology (USgFNAC) (1).

US uses reflected high frequency sound waves. By electric transformation and (frequently) computerized processing, the reflected sound waves are transformed into a two dimensional image. Tissue characterisation with the use of US has been studied, but reliable differentiation between malignant and benign lesions was never shown. This changed with the US guided fine needle aspiration cytology. This technique of diagnosing tumor cells in lymph nodes appears to be very reliable in well trained hands. However, the accuracy of this technique depends fully on the skills of the investigator (6).

In the studies presented in this thesis the patients underwent PET, MRI and/or CT. The MRI studies were performed on a 1.5 Tesla Philips Gyroscan S-15 (Philips, Eindhoven, The Netherlands). T1-(TR = 650 msec, TE = 20 msec) and T2-(TR = 2000 msec, TE = 50-100 msec) weighted pulse sequences were obtained. A head coil was used to obtain axial and coronal slices with a slice thickness varying between 3-5 mm.

The CT scanner was a Philips Tomoscan SR (Philips, Eindhoven, The Netherlands). Axial and coronal slices were made with a slice thickness varying between 5-10 mm. Intravenous contrast medium (Telebrix<sup>R</sup> 350) was administered to all of these patients.

The radiologic criteria used to assess cervical metastases in patients with a primary SCC were for MRI and CT the same (6,7).

1. Nodes with a minimal axial diameter of 11 mm or more in the subdiaphragmatic region and 10 mm or more in the other lymph node-bearing regions were considered metastatic;
2. Groups of three or more lymph nodes of 9 or 10 mm in the subdiaphragmatic region, and of 8 or 9 mm in the other lymph node drainage regions of the tumor were considered metastatic;
3. All nodes that showed irregular enhancement on MRI and were surrounded by a rim of enhancing viable tumor or lymph node tissue were considered metastatic.

**Figure 4.** The radiologic criteria according to van den Brekel (6,7).

With the clinical introduction of PET a new way of cancer imaging was introduced. The transition from slowly growing and well differentiated to rapidly growing and poorly differentiated neoplasms is accompanied by a progressive increase in the protein and glucose metabolism (8). The increased metabolism can be visualized by PET with the use of radioactive tracers. The increased glycolysis can be visualized with FDG. The non-

carrier-added glucose analogue FDG was synthesized with a radiochemical purity better than 98% (9). The increased protein synthesis could be reflected with the use of carboxyl-labeled TYR (10). Initially, TYR was produced through the isocyanide route with a radiochemical purity of more than 99% and a specific activity of more than 3.7 GBq/micromole. To increase the production yield at a later time, remote controlled synthesis of non-carrier-added TYR through a microwave induced Bücherer-Strecker synthesis was developed.

The PET camera used was a Siemens ECAT 951 whole-body machine. The device acquires 31 planes over an axial length of 10.8 cm. The measured resolution of the system is 6 mm full width at half maximum (FWHM) transaxially in the center of the field of view.

### **2.6 Definition of quantitative parameters**

To compare the different data of the imaging modalities, various statistical measures can be used. The sensitivity was calculated by dividing the number of true-positive cases by the sum of the number of true-positive cases and the number of false-negative cases (100%). The specificity was calculated by dividing the number of true-negative cases by the sum of the number of true-negatives and false positives (100%). The positive predictive value was calculated by dividing the number of true-positives by the sum of the number of true-positives and false-positives (100%). The negative predictive value was calculated by dividing the number of true-negatives by the sum of the number of true-negatives and false-positives (100%). The accuracy (validity) was calculated by dividing the sum of the true-positives and true-negatives by the total number of lymph nodes (100%). The false-negative rate was calculated by dividing the false-negatives by the sum of false-negatives and true-negatives (100%). The false positive rate was calculated by dividing the false-positives by the sum of true-positives and false-positives (100%) (11).

**References**

1. Van den Brekel MWM. Assessment of lymph node metastases in the neck. Thesis Free University Amsterdam, (Utrecht: Elinkwijk) 1992.
2. Rouvière H. Anatomie des lymphatiques de l'homme. Paris: Masson et cie, 1932.
3. Sobin LH, Wittekind Ch, eds. International Union Against Cancer. TNM classification of malignant tumours, 5th edition. New York: Wiley & Sons , 1997.
4. Beahrs OH, Henson DE, Hutter RP, Meyers MH, eds. American Joint Committee on Cancer (AJCC). Manual of staging of cancer, 3rd edition. Philadelphia: JB Lippincott Company, 1988
5. Robbins KT, Medina JE, Wolfe GT, Levine PA. Sessions RB, Pruet CW. Standardizing neck dissection terminology. Arch Otolaryngol Head Neck Surg 1991;117:601-605.
6. Van den Brekel MWM, Castelijns JA, Stel HV, et al. Modern imaging techniques and ultrasound-guided aspiration cytology for the assessment of neck node metastases: a prospective comparative study. Eur Arch Otorhinolaryngol 1993;250:11-17.
7. Van den Brekel MWM, Stel HV, Castelijns JA, et al. Cervical lymph node metastasis: assessment of radiologic criteria. Radiology 1990;177:379-384.
8. Warburg O. The metabolism of tumors. London: Arnold Constable 1930;75-327.
9. Hamacher K, Coenen HH, Stocklin G. Efficient stereospecific synthesis of no-carrier-added 2-<sup>[18F]</sup>-fluoro-2-deoxy-D-glucose using aminopolyether supported nucleophilic substitution. J Nucl Med 1986;27:235-238.
10. Ishiwata K, Kubota K, Murakami M, et al. Re-evaluation of amino acid-pet studies: can the protein synthesis rates in the brain and tumor tissues be measured in vivo ? J Nucl Med 1993;34:1936-1943.
11. Dawson-Saunders B, Trapp RG. Basic and clinical biostatistics. East Norwalk: Appleton & Lange, 1990.





- CHAPTER 3 -

DETECTION OF LYMPH NODE METASTASES OF SQUAMOUS CELL  
CANCER OF THE HEAD AND NECK  
WITH FDG-PET AND MRI

Jan Willem Braams, Jan Pruim, Nicole J.M. Freling, Peter G.J. Nikkels,  
Jan L.N. Roodenburg, Geert Boering, Willem Vaalburg and Albert Vermey

Departments of:    Oral and Maxillofacial Surgery  
                          PET Center  
                          Diagnostic Radiology  
                          Pathology  
                          Surgical Oncology

Groningen University Hospital, Groningen, The Netherlands

The uptake of 2-deoxy-2-[<sup>18</sup>F]fluoro-D-glucose (FDG) in neck lymph nodes of twelve patients with a squamous cell carcinoma of the oral cavity was studied with PET in order to detect and locate lymphogenic metastases. **Methods:** The results of FDG-PET imaging were compared with clinical, MRI and histopathologic findings. Standardized uptake values (SUV) were also calculated. **Results:** A sensitivity of 91% and a specificity of 88% were calculated for FDG-PET. In contrast, a sensitivity of 36% and a specificity of 94% were calculated for MRI. Calculated SUVs for reactive lymph nodes, metastatic lymph nodes and the primary tumor were undifferentiated. **Conclusion:** Using FDG-PET, lymph node metastases of squamous cell carcinomas of the oral cavity can be visualized with a high sensitivity and specificity. FDG-PET can be an improvement in the evaluation of the neck.

## Introduction

It is difficult to assess the presence of cervical lymph node metastases of squamous cell carcinomas of the upper aero-digestive tract in a clinically negative neck. However, there is clinical relevance in detecting such occult metastases, since the extent of the treatment is determined by the size of the tumor and by the presence or absence of metastatic lymph nodes. Many institutions employ elective neck treatment if the risk of occult metastases is estimated to be higher than 15% to 20% (1). Imaging techniques such as US, MRI and CT have improved the staging of the neck as compared to palpation. These modalities monitor tumors or lymph node metastases by size and structural changes, not by metabolic activities. The overall error rate of assessing the presence or absence of cervical lymph node metastasis by palpation is 20%-28%, while for CT figures range from 7.5% to 28% and for MRI 16% is reported (1,2). Consequently, there is a great need for an improved method that allows the detection of lymphogenic metastases in the neck, particularly in the clinically negative neck ( $N_0$ ). It is expected that alterations in metabolism precede structural alterations and that registration of these alterations may improve the detection of metastases. A high rate of glycolysis is the biochemical hallmark of many types of tumors, a phenomenon first described by Warburg, and confirmed by others (3). The transition from slowly growing and well-differentiated to rapidly growing and poorly differentiated neoplasms is accomplished by a progressive increase in anaerobic glycolysis. The increased glycolysis can be monitored with PET, using the glucose analogue 2-deoxy-2-[ $^{18}$ F]fluoro-D-glucose (FDG) (4). Several investigators have applied FDG-PET in detection and staging of different types of cancer. Haberkorn et al. investigated the uptake of FDG in relation to the proliferation rate of head and neck tumors and found two groups of patients with different uptake patterns (5). The uptake of FDG in malignant head and neck tumors and metastases was studied by Minn and co-workers. They found that FDG uptake is associated with the proliferative activity of the tumor (6). Jabour et al.(7) found that the normal head and neck anatomy could be delineated with FDG-PET. They also found that non-enlarged lymph nodes, negative for metastatic disease according to MRI and CT, may be detected by FDG-PET.

However, FDG is also accumulated in abscesses as described by Tahara et al.(8) and Sasaki et al.(9). Moreover, accumulation in macrophages and newly formed granulation tissue around the tumor is mentioned by Kubota et al.(10). This can be a major problem which may influence the specificity and sensitivity of FDG-PET in detecting lymph node metastases.

The aim of this study is to investigate the usefulness of FDG-PET in the identification of lymph node metastases of squamous cell carcinomas of the oral cavity, compared to analysis of clinical, magnetic resonance imaging and histopathologic findings.

## Materials and methods

### Patients

Twelve patients were submitted to the Head and Neck Cooperative Oncology Group of the University Hospital Groningen for evaluation of squamous cell carcinoma of the upper aero-digestive tract. One patient had a primary tumor of the upper gingiva-/retromaxillary area, one patient of the upper buccogingival sulcus, one patient of the lower gingiva, one patient of the lower lip, five patients of the floor of the mouth and three patients of the oral tongue (Table 1). Staging of the tumor and metastases were based on the International Union Against Cancer (UICC, 1987) and American Joint Committee on Cancer (AJC, 1988) TNM-classification. Histological grading of the primary tumor and metastases was done according to the WHO (1978) classification (11). There were no diabetic patients in our series. The patients were allowed a light low-glucose breakfast 3-4 hrs before the PET study. Written informed consent was obtained in all patients and the study was approved by the Medical Ethics Committee of the University Hospital Groningen.

### PET Imaging

No-carrier-added FDG was synthesized with a radiochemical purity greater than 98% according to Hamacher et al. (12).

The PET camera used was a Siemens ECAT 951 whole-body machine. The device acquires 31 planes over an axial length of 10.8 cm. The measured resolution of the system is 6 mm full width at half maximum (FWHM) transaxially in the center of the field of view.

To prevent overlapping of anatomical structures and movements of the head during the study, a foam-filled head mould was made for each patient. The patient's head was positioned in this head mould with the Frankfurter horizontal plane making an angle of 110° with the horizontal bed position. The Frankfurter horizontal plane is defined as a fictive line between the external meatus of the ear canal and the lower orbital rim. This position was reached by asking the patient to stretch the neck by moving the head backwards. To allow anatomical orientation on the PET images, small radioactive markers were placed on the tip of the chin, the mandibular angles, the mid-line of the clavicles and the jugulum. Next, two transmission scans of 15 min each, were performed: a cranial one and a caudal one. The total distance was 21 cm. Immediately after the second transmission scan, FDG (185 MBq to 370 MBq) was injected into a peripheral vein of the upper extremity. Data acquisition was started 30 min after injection. Two static emission scans were made of ten min each in reverse order as compared to the transmis-

sion scans. Any visually positive hot spot on each emission scan was considered to be a metastatic lymph node.

**Table 1.** The assessment of lymph node metastases of squamous cell carcinomas of the oral cavity.

Patient Nr(sex,age)	Tumor Stage, location ‡	Metastases *				Neck Treatment †
		Clinical R / L	PET R / L	MRI R / L	Hist R / L	
1 (m,66)	T3N0 , oral tongue R	- / -	++ / -	+ / +	++ / -	MRND / -
2 (m,48)	T4N2b, buc ging sulc L	- / ++	- / ++	- / ++	- / ++	- / MRND
3 (f,79)	T1N1 , lower lip L	- / +	- / +	- / -	- / +	- / SOND
4 (m,59)	T4N2a, retro maxil. R	+ / -	++ / +	+ / -	++ / +	MRND / SOND
5 (m,74)	T4N0 , lower gum L	- / -	++ / ++	- / ++	- / -	SOND / MRND
6 (f,51)	T2N2a, floor mouth R	+ / -	++ / +	+ / -	++ / -	MRND / -
7 (f,66)	T2N0 , oral tongue R	+ / -	++ / -	+ / -	++ / -	SOND / -
8 (m,73)	T2N3 , floor mouth L	+ / +	+ / +	+ / +	- / -	SOND / MRND
9 (m,62)	T1N0 , floor mouth R	- / -	- / -	- / -	- / -	SOND / _
10 (m,67)	T4N0 , floor mouth RL	- / -	++ / ++	++ / -	++ / +	SOND / SOND
11 (m,62)	T2N0 , floor mouth L	- / -	- / ++	- / ++	- / +	- / SOND
12 (f,85)	T4N0 , oral tongue L	- / -	- / +	- / -	- / +	SOND / SOND

\* The clinical, PET, MRI, and histopathological staging of both sides of the neck (- = no suspicious nodes, + = one suspicious node, ++ = two or more suspicious nodes). † The neck treatment that has taken place (- = no treatment, SOND = supraomohyoid neck dissection, MRND = modified radical neck dissection). ‡ The T- and N- stage according to the UICC (1987) and AJCC (1988) classifications of the primary tumor and location. Buc ging sulc = upper bucco gingival sulcus

### MRI

MRI was performed with a 1.5 Tesla Philips Gyroscan S-15 in all patients. T1-(TR = 650 msec, TE = 20 msec) and T2-weighted (TR = 2000 msec, TE = 50, 100 msec) pulse sequences were obtained. Using a head coil, axial and coronal slices were made with slice thickness varying between 3 - 5 mm. The following radiologic criteria (2) for assessing cervical metastases in patients with a primary squamous cell carcinoma were used:

1. Nodes with a minimal axial diameter of 11 mm or more in the subdigastic region and 10 mm or more in the other lymph node-bearing regions were considered metastatic.
2. Groups of three or more lymph nodes of 9 or 10 mm in the subdigastic region, and of 8 or 9 mm in the other lymph node drainage regions of the tumor were considered metastatic.
3. All nodes, irrespective of size, that showed irregular enhancement on MRI and that were surrounded by a rim of enhancing viable tumor or lymph node tissue were considered metastatic (2).

### Histopathology

Shortly after the PET and MRI studies, radical surgery of the primary tumor and a selective or modified radical neck dissection was performed. The removed specimen was stretched out on a polystyrene pad and the coordinates were marked immediately after removal by using colored pins. From the specimens, the lymph nodes were isolated and studied individually using hematoxylin-eosin staining. The largest diameter was examined from each lymph node. Lymph nodes with a diameter of 2 cm or more were also examined.

### Analysis of data

The transversal PET images were individually reoriented to sagittal and coronal planes in order to obtain a better view of the lymph nodes. The images were analysed visually by two observers at the same time. The number and location of the tumor positive nodes

were assessed. Regions of interest (ROI) were drawn on hot-spots representing the area of highest accumulation. Also, ROIs were placed over areas representing areas of normal tissue. Tracer accumulation was measured using the standardized uptake values (SUV):

$$\text{SUV} = \frac{\text{Radioactivity conc in ROI [mCi cm}^{-3}\text{]}}{\text{Injected dose [mCi]/Body weight [g]}}$$

Unpaired Student's t-tests were used to compare the SUVs of the metastases with those of the reactive lymph nodes and those of the normal tissue, respectively. A similar approach was done for the MRI. The PET and MRI observers were unaware of the results of each other's techniques and of the histopathology. Using histopathology as the gold standard, specificity, sensitivity and predictive values of a positive and a negative test were calculated for the lymph nodes detected by PET and MRI. Calculations also were made for the justification of a therapeutical neck dissection using histopathology as a reference.

Sensitivity was calculated by dividing the number of true-positive cases by the sum of the number of true-positive cases and the number of false-negative cases (x 100%). The specificity was calculated by dividing the number of true-negative cases by the sum of the number of true-negative and false-positives (x 100%). The positive predictive value was calculated by dividing the number of true-positives (x 100%). The negative predictive value was calculated by dividing the number of true-negatives by the sum of the number of true-negatives and false-positives (x 100%). The accuracy (validity) was calculated by dividing the sum of the true-positives and true-negatives by the total of number of lymph nodes (x 100%). The false-negative rate was calculated by dividing the false-negatives by the sum of false-negatives and true-negatives (x 100%). The false-positive rate was calculated by dividing the false-positives by the sum of true-positives and false-positives (x 100%) (13).

## Results

Twelve patients (8 male and 4 female) with histologically verified primary squamous cell carcinomas of the mucosa of the oral cavity and a staging of the neck N<sub>0</sub>-N<sub>3</sub> were studied (mean age 65.3, s.d. 10.4 yr). Patient characteristics are summarized in Table 1.

Histopathology of the resection specimens showed 22 metastatic lymph nodes, 25 reactive lymph nodes and 152 normal lymph nodes. PET gave 42 positive lymph nodes. Twenty of the 22 metastatic lymph nodes, and 16 of the 25 reactive lymph nodes had a positive PET signal. In addition, six lymph nodes which showed up on FDG-PET were normal on histopathological examination (Table 2). The smallest metastatic lymph node detected was 4 mm. The two metastatic lymph nodes not detected were 2.5 and 3 mm in size, respectively. The metastatic lymph nodes had a SUV of  $2.5 \pm 0.8$ . The SUV of the reactive lymph nodes was  $2.6 \pm 1.4$  and that of the ROIs placed over the areas of normal tissue was  $1.0 \pm 0.3$ . The metastatic SUVs and reactive SUVs differed significantly from normal tissue ( $p < 0.001$ ), but there was no significant difference between metastatic and reactive SUVs ( $p = 0.7$ ).

**Table 2.** The results of PET, MRI and histopathology in the detection of lymph node metastases of squamous cell carcinomas of the oral cavity.

	Histopathology			
	metastatic	reactive	normal	total
PET positive	20	16	6	42
PET negative	2	9	146	157
total	22	25	152	199
MRI positive	8	2	8	18
MRI negative	14	23	144	181
total	22	25	152	199

As can be seen in Figure 1 of the SUVs of the reactive lymph nodes fall apart into two clusters. No histological difference between the two clusters was established. MRI showed 18 positive lymph nodes. When compared with the histopathological results, 8



lymph nodes were metastatic and 2 lymph nodes were reactive. Finally, 8 of the lymph nodes detected on MRI were normal on histological examination (Table 2). No nodes with irregular enhancement smaller than 10 mm were found. The smallest metastatic lymph node detected was 10 mm in size.

Sensitivity, specificity and predictive value of a positive and negative test and the false-positive rate were calculated for both diagnostic modalities and are summarized in Table 3.

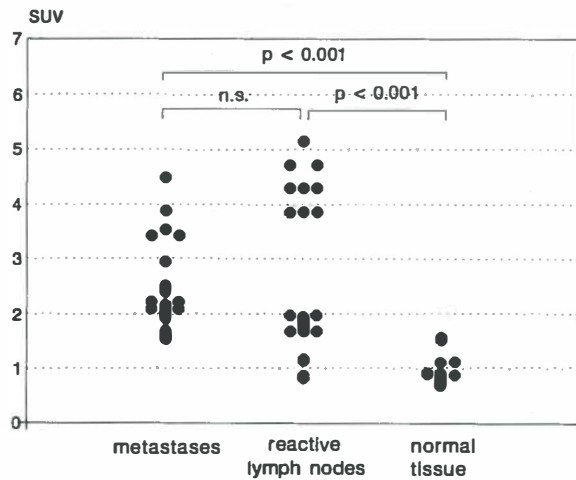


**Figure 1.** The uptake of FDG, measured as SUV, as compared to the histopathological findings of metastases, reactive lymph nodes and normal tissue in the head and neck region. ns = not significant.

## CHAPTER 3

---

**Table 3.** Sensitivity, specificity and Positive and Negative predictive value and false positive rate for FDG-PET and MRI.

	PET	MRI
Sensitivity	91%	36%
Specificity	88%	94%
Positive predictive value	48%	44%
Negative predictive value	99%	92%
False positive rate	52%	55%

According to the FDG-PET data, a neck dissection was justified in all cases with metastatic disease. According to the MRI data, a neck dissection was not justified in 4 patients (false negative). According to the FDG-PET data in 5 patients an unnecessary neck dissection should have taken place (false positive). In comparison with MRI 4 patients would have been operated upon unnecessarily (Table 4).

**Table 4.** The results of PET, MRI and Histopathology in the justification of therapeutic neck dissections of squamous cell carcinoma of the oral cavity.

	Histopathology		
	positive neck	negative neck	total
PET positive	10	5	15
PET negative	0	9	9
total	10	14	24
MRI positive	7	4	11
MRI negative	4	9	13
total	11	13	24

## Discussion

The application of PET, using the tracer FDG, is a promising complementary diagnostic tool in the management of patients with cancer. Several authors have mentioned the

uptake of FDG in lymph node metastases (5-7,14-18). One study described the detection of tumor recurrence in a previously irradiated metastasis of breast cancer. In this study, FDG-PET was the first method that detected the tumor recurrence (15). Minn et al. described the uptake of FDG in malignant head and neck tumors and metastases (6). However, the tumor population in their study was inhomogeneous with respect to histology. Haberkorn et al. investigated the uptake of FDG in relation to the proliferation rate of squamous cell carcinomas of the head and neck (5). They found that the glucose uptake could be correlated with the proliferative activity of the tumor or metastases. Wahl et al. reported that FDG given intravenously has potential as radiopharmaceutical agent for detection of metastatic tumors in regional lymph nodes using PET scanning (18). In a basic study in mice and rats, Brown et al. investigated the intratumoral distribution of tritiated 2-fluoro-2-deoxy-D-glucose (2-DG) and  $^{14}\text{C}$ -2-deoxy-D-glucose ( $^{14}\text{C}$ -DG) by autoradiography and found a selective accumulation of 2-DG in viable cancer cells and a negligible concentration of 2-DG in necrotic areas (19). However, FDG also accumulates in inflammatory tissue and in abscesses (8-10), which limits the value of this tracer in the detection of tumor tissue. In our study we investigated the clinical applicability of FDG-PET in the detection of lymph node metastases of squamous cell carcinomas of the oral cavity. The detection of these metastases, especially metastases not yet detected with conventional techniques such as palpation, MRI, CT or US, and the exact staging will have grave implications for treatment.

The results of FDG-PET were compared with MRI; histopathology of the removed specimens was used as reference.

PET concurred with histopathology in 20 of 22 cases of metastatic lymph nodes. The 2 metastatic lymph nodes which were not detected by FDG-PET can be attributed to the small diameter of the metastatic lymph nodes (2 mm and 3.5 mm) in relation to the resolution of the camera used.

It can also be argued that these metastases were not delineated from the surrounding normal tissue due to low glycolytic activity. Minn et al. (15) suggested the same explanation for the breast tumor metastases which were not detected by FDG-PET. The relatively low glycolytic activity has also been demonstrated for low grade gliomas (20) and metastases of thyroid cancer (16). Finally, it also can be argued that a low SUV in relation with the partial volume effect resulted in missing these small lymph nodes.

The smallest metastatic lymph node detected by FDG-PET was 4 mm whereas with

MRI the smallest detected metastatic lymph node was 10 mm. Nodes with irregular enhancement smaller than 10 mm were not found in our study. A major problem with the radiologic criteria used is when a lymph node shows no irregular enhancement on MRI that lymph node would be considered metastatic on the sole criterion of size as described by Van den Brekel et al. They consider 9-10 mm in the subdigastric region and 10-11 mm in the other lymph node drainage regions as the critical size to differentiate between metastases or reactive lymph nodes (2). As a consequence, specificity of this technique is increased but at the cost of lowering the sensitivity, since smaller lymph nodes with no irregular enhancement are excluded by definition. Eight lymph nodes not detected by MRI but positive with FDG-PET showed metastatic cancer on histopathology. Jabour et al. investigated the normal FDG-PET anatomy of the head and neck area, and used this information to study 12 patients with oral cancer (7). Similar to our study, they found that nonenlarged lymph nodes, negative on MRI and CT can be detected by FDG-PET. In contrast to our study they detected only 25 of 34 metastatic lymph nodes with FDG-PET. This indicates a sensitivity of 74% in their series (6), whereas we found a sensitivity of 91%. This difference should probably be explained by the small group of patients of both studies.

A major problem with FDG-PET is the differentiation between reactive and metastatic lymph nodes. In this study FDG-PET also detected 16 of 25 reactive lymph nodes that were present in the specimens. This relatively high false-positive rate is probably due to the accumulation of FDG in inflammatory tissue. Unfortunately, the SUVs calculated for the suspected lymph nodes showed no differences between reactive and metastatic lymph nodes, thus providing no additional value.

We found a total of 199 lymph nodes in 17 dissection specimens. Most likely, this relatively low number of lymph nodes should be explained by the different operation techniques of the neck dissections. Eleven of the 17 neck dissections were supraomohyoid neck dissections and 6 were modified radical neck dissections. Another explanation may be that the smaller lymph nodes are missed in the histopathological examination of the specimens. Whatever the reason, the small number of lymph nodes found in the resection specimens must make us aware that the calculated specificity, in contrast to the sensitivity, is not a hard figure. The specificity depends highly on the number of lymph nodes retrieved from the specimens.

In order to avoid this drawback we have looked at the justification for neck dissec-

tion by FDG-PET and MRI respectively. In our institution elective neck treatment is justified in T<sub>4</sub> squamous cell carcinoma of the lip or T<sub>2-4</sub> squamous cell carcinomas of the oral cavity. Neck treatment is obligatory by the detection of one suspicious node found by clinical examination, MRI or PET. Using these criteria, a calculation was made between FDG-PET, MRI and histopathology.

With FDG-PET, in 19 of the 24 necks (79%) a correct decision would have been made for justifying an operation or not. According to the MRI data, 16 of 24 necks (66%) a correct decision would have been made. In case FDG-PET was used as a reference 5 necks would have been operated unnecessarily. According to the MRI-data 4 negative necks would have been operated, while 4 other (positive) necks would not have been operated. Most important, with FDG-PET no false-negative decisions should have been made. These data show that FDG-PET can be an important diagnostic modality in the assessment of metastases of squamous cell carcinomas of the neck.

The TNM-classification of staging of the head and neck region is still based on palpation. According to the histopathology, the TNM-staging of the head and neck region by palpation was understaged in seven patients, well staged in four patients and overstaged in one patient. If the TNM-staging would have been based on the FDG-PET results, no patients would have been understaged, nine patients well-staged and three patients overstaged compared with the histopathological results.

The additional value of FDG-PET can also be concluded from the following. We studied nine elective neck dissections which were clinically staged N<sub>0</sub>. In this group, there were nine metastatic nodes. All these nodes were detected with PET, a sensitivity of 100% and a specificity of 89%. In comparison, using MRI, Van den Brekel et al. studied 60 elective neck dissections which were clinically staged N<sub>0</sub>. In this group of neck dissections there were 25 pathological nodes. Fifteen of these nodes were detected by MRI, a sensitivity of 60% and a specificity of 89%. They concluded that MRI can improve the preoperative staging of cervical lymph nodes (1), but our results indicate that FDG-PET can be a better modality for that purpose.

In one patient, we found a contralateral hot spot, which at the time of primary treatment was not surgically removed because the location was thought to be unrelated to the primary tumor. Six months after the operation, the patient developed a metastatic lymph node at that location and underwent subsequent surgery.

A method to improve the relatively high false-positive rate of PET in the detection of lymph node metastases of squamous cell carcinoma of the upper aerodigestive tract is desired. A recent animal study of Kubota et al. suggests that a possible differentiation can be made between tumor and reactive tissue, based on different uptake patterns (21). This may also reduce the high false-positive rate in the assessment of lymph nodes. It is possible that PET in combination with a protein synthesis rate (PSR) marker, as L-[1- $^{11}\text{C}$ ]-tyrosine (22,23) or a DNA-synthesis rate marker, e.g.  $^{11}\text{C}$ -thymidine, will decrease the false positive rate (24). Leskinen-Kallio et al. reported the uptake of L-[ $^{11}\text{C}$ ]-methionine in cervical nodal metastases in four patients. In their study, clinical evidence of regional metastatic spread was available in seven patients. but in three patients the metastatic nodes were outside the field of view. They concluded that head and neck cancers of varying histology can be imaged with L-[ $^{11}\text{C}$ ]-methionine (25). It has to be realized that L-[ $^{11}\text{C}$ ]-methionine does not reflect the PSR due to the complicated metabolic degradation pattern of this tracer and the fact that this aminoacid partially reflects the transport system in brain and tumor tissues (26). The value of  $^{11}\text{C}$ -labeled amino acids for the detection of tumor tissue still has to be established.

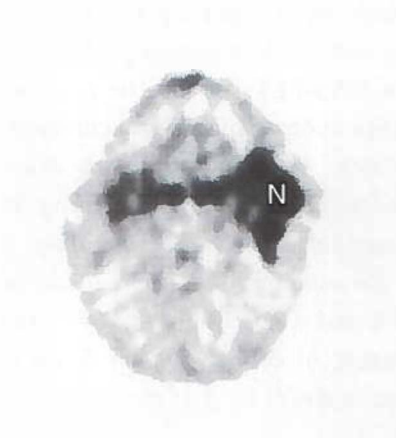


**Figure 2.** FDG-PET image of patient 2. A  $T_4N_2b$  carcinoma of the oral cavity. On the right side three submandibular lymph nodes (N). These nodes were histologically positive.

We conclude that FDG-PET imaging detects metastases of squamous cell carcinomas of the oral cavity with high sensitivity and specificity. However, the false-positive rate of FDG-PET imaging is relatively high. The results of this study indicate that FDG-PET imaging can improve the assessment and staging of neck metastases.

### References

1. Van den Brekel MWM, Castelijns JA, Croll GA, et al. Magnetic resonance imaging vs. palpation of cervical lymph node metastases. *Arch Otolaryngol Head Neck Surg* 1991;117:666-673.
2. Van den Brekel MWM, Stel HV, Castelijns JA, et al. Cervical lymph node metastasis: assessment of radiologic criteria. *Radiology* 1990;177:379-384.
3. Warburg O. *The metabolism of tumors*. London: Arnold Constable 1930;75-327.
4. Strauss LG, Conti PS. The applications of PET in clinical oncology. *J Nucl Med* 1991;32:623-648.
5. Haberkorn U, Strauss LG, Reisser Ch, et al. Glucose uptake, perfusion and cell proliferation in head and neck tumors: relation of positron emission tomography to flow cytometry. *J Nucl Med* 1991;32:1548-1555.
6. Minn H, Joensuu H, Ahonen A, Klemi P. Fluorodeoxyglucose imaging: a method to assess the proliferative activity of human cancer in vivo. *Cancer* 1988;61:1776-1781.
7. Jabour BA, Choi Y, Hoh CK, et al. Extracranial head and neck: PET imaging with 2-[F-18]Fluoro-2-Deoxy-D-Glucose and MR Imaging correlation. *Radiology* 1993;186:27-35.
8. Tahara T, Ichiya Y, Kuwabara Y, et al. High [<sup>18</sup>F]fluorodeoxyglucose uptake in abdominal abscesses: a PET study. *J Comput Assist Tomogr* 1989;13:829-831.
9. Sasaki M, Ichiya Y, Kuwabara Y, et al. Ringlike uptake of [<sup>18</sup>F]FDG in brain abscess: a PET study. *J Comput Assist Tomogr* 1990;14:486-487.
10. Kubota R, Yamada S, Kubota K, Ishiwata K, Tamahashi N, Ido T. Intratumoral distribution of fluorine-18-fluorodeoxyglucose in vivo: High accumulation in macrophages and granulatio-n tissues studied by microautoradiography. *J Nucl Med* 1992;33:1972-1980.
11. Shanmugaratnam K, Sobin LH. *Histological typing of upper respiratory tract tumors*. Geneva: World Health Organization, 1978.
12. Hamacher K, Coenen HH, Stocklin G. Efficient stereospecific synthesis of no-carrier-added 2-[<sup>18</sup>F]-fluoro-2-deoxy-D-glucose using aminopolyether supported nucleophilic substitution. *J Nucl Med* 1986;27:235-238.
13. Dawson-Saunders B, Trapp RG. *Basic and clinical biostatistics*. East Norwalk, Appleton & Lange, 1990.
14. Chen BC, Hoh C, Choi Y, et al. Evaluation of primary head and neck tumor with PET-FDG. *Clin Nucl Med* 1990;15:758.
15. Minn H, Soini I. [<sup>18</sup>F]Fluorodeoxyglucose scintigraphy in diagnosis and follow up of treatment in advanced breast cancer. *Eur J Nucl Med* 1989;15:61-66.
16. Joensuu H, Ahonen A. Imaging of metastases of thyroid carcinoma with fluorine-18 fluoro-deoxyglucose. *J Nucl Med* 1987;28:910-914.
17. Nagata Y, Yamamoto K, Hiraoka M, et al. Monitoring liver tumor therapy with [<sup>18</sup>F]FDG



- positron emission tomography. *J Comput Assist Tomogr* 1990;14:370-374.
18. Wahl RL, Kaminski MS, Ethier SP, Hutchins GD. The potential of 2-deoxy-2-[<sup>18</sup>F]fluoro-D-glucose (FDG) for the detection of tumor involvement in lymph nodes. *J Nucl Med* 1990;31:1831-1835.
  19. Brown RS, Fisher SJ, Wahl RL. Autoradiographic evaluation of the intratumoral distribution of 2-deoxy-D-glucose and monoclonal antibodies in xenografts and human ovarian adenocarcinoma. *J Nucl Med* 1993;34:75-82.
  20. Di Chiro G. Positron emission tomography using [<sup>18</sup>F]fluorodeoxyglucose in brain tumors: a powerful diagnostic and prognostic tool. *Invest Radiol* 1986;22:360-371.
  21. Kubota R, Kubota K, Yamada S, Tada M, Ido T, Tamahashi N. Microautoradiographic study for the differentiation of intratumoral macrophages, granulation tissues and cancer cells by the dynamics of fluorine-18-fluorodeoxyglucose uptake. *J Nucl Med* 1994;35:104-112.
  22. Deamen BJG, Elsinga PH, Ishiwata K et al. A comparative PET study using different <sup>11</sup>C-labelled amino acids in Walker 256 carcinosarcoma-bearing rats. *J Nucl Med Biol* 1990;18:197-204.
  23. Willemsen ATM, van Waarde A, Elsinga PH, et al. Protein synthesis rate determined in oncological patients with L-[1-<sup>11</sup>C]Tyrosine. *J Nucl Med* 1993;34:183p.
  24. Eijkeren van ME, Schryver de A, Goethals P, et al. Measurement of short-term <sup>11</sup>C-thymidine activity in human head and neck tumours using positron emission tomography (PET) *Acta Odontol* 1992;31:539-543.
  25. Leskinen-Kallio S, Någren K, Lehtikainen P, Ruotsalainen U, Teräs M, Joensuu H. Carbon-11-methionine and PET is an effective method to image head and neck cancer. *J Nucl Med* 1992;33:691-695.
  26. Ishiwata K, Kubota K, Murakami M, et al. Re-evaluation of amino acid-PET studies: Can the protein synthesis rates in the brain and tumor tissues be measured in vivo. *J Nucl Med* 1993;34:1936-1943.



- CHAPTER 4 -

NODAL SPREAD OF SQUAMOUS CELL CARCINOMA OF THE ORAL  
CAVITY DETECTED WITH PET-TYROSINE, MRI AND CT

Jan Willem Braams, Jan Pruijm, Peter G.J. Nikkels, Jan L.N. Roodenburg,  
Willem Vaalburg and Albert Vermey

Departments of:    Oral and Maxillofacial Surgery  
                         Pathology  
                         Surgical Oncology  
                         PET Center

Groningen University Hospital, Groningen, The Netherlands

The uptake of L-[1-<sup>11</sup>C]-tyrosine (TYR) in cervical lymph nodes of eleven patients with squamous cell carcinoma (SCC) of the oral cavity was studied with PET to detect lymphogenic metastases. **Methods:** The TYR-PET results were compared with clinical, MRI, CT, histopathologic findings and historical data of patients studied with FDG. Sensitivity, specificity, accuracy and the positive and negative predictive values were calculated. **Results:** TYR-PET had sensitivity of 83% and a specificity of 95%. In contrast, the sensitivity and specificity for MRI were 33% and 96%, respectively. The sensitivity and specificity for CT were 55% and 91%, respectively. TYR-PET results compared favorably with FDG. **Conclusion:** With TYR-PET, SCC metastases of the oral cavity can be visualized with high sensitivity and specificity. TYR-PET can be an additional tool for further evaluation of neck malignancies.

## Introduction

The assessment of the presence of cervical lymph node metastases of squamous cell carcinomas (SCCs) of the oral cavity in a "clinically negative neck" is difficult. Detecting such occult metastases is clinically important, since the extent of the treatment is determined by tumor size and the presence or absence of metastatic lymph nodes.

Available imaging techniques such as MRI, CT and US have improved tumor staging of the neck as compared to palpation. With these techniques, it is possible to monitor tumors and metastases by size and structural changes and not by metabolic activities. The overall error rate of assessing the presence or absence of cervical lymph node metastases by palpation is 20%-28%, error rate 7.5%-28% for CT and is 16% for MRI (1,2). Consequently, an imaging modality that can detect nodal metastases with high sensitivity and specificity is useful for accurate treatment planning of head and neck cancer.

An alternative way of cancer imaging is to use the physio-chemical properties of tumor cells. For instance, it has been shown that malignant cells have an increased glucose consumption due to an increased glycolysis (3). Based on these findings, various investigators have applied 2-deoxy-2-[<sup>18</sup>F]fluoro-D-glucose (FDG) as a marker of tumor tissue in PET. Although FDG-PET imaging of SCC may be useful in detecting nodal metastases in the neck (4), it is hampered by high false-positive rates due to FDG accumulation in inflammatory tissues (5). We have found similar limitations (4).

As an alternative, some centers have started to use <sup>11</sup>C-labeled amino acids, mainly methyl-labeled <sup>11</sup>C-methionine. Lindholm et al. (6) studied L-[methyl-<sup>11</sup>C] methionine (MET) uptake in patients with head and neck cancer and found that MET is useful in PET imaging of head and neck cancer. Ishiwata et al. (7), however, found that MET visualized amino acid transport phenomenon rather than found protein synthesis rates. We used the carboxyl-labeled amino acid tyrosine, L-[1-<sup>11</sup>C]-tyrosine (TYR) because it is possible to reflect the protein synthesis rate in cancer cells with TYR. So far, TYR has been successfully used in rats and humans to visualize different tumors and to quantitate protein synthesis rates (8,9).

The aim of this study was to investigate whether cervical nodal spreading of SCC of the oral cavity can be visualized with TYR-PET and to compare these results with the clinical, MRI, CT and histopathologic findings. Also, a comparison was made with historic data from a group of patients studied with FDG (4).

## Materials and Methods

### Patients

Eleven patients (7 men, 4 women; mean age 62.3 yr) who underwent treatment of a SCC of the oral cavity were studied (Table 1). In all patients, there was an indication for a therapeutic or elective neck dissection. None of the patients received preoperative radiotherapy or chemotherapy. The study was approved by the Medical Ethics Committee of the University Hospital Groningen. Before entrance into the study, written informed consent was obtained from all patients. The characteristics of the 12 patients who had previous FDG studies have been previously published (4).

Staging of the tumor and its metastases was based on the International Union against Cancer (UICC, 1992) and American Joint Committee on Cancer (AJC, 1988) TNM classification. Histological typing of the primary tumor and metastases was performed according to the WHO (1978) classification (10).

### Tracer Synthesis

Initially, L-[1-<sup>11</sup>C]-tyrosine was produced through the isocyanide route as described by Bolster et al. (11) with a radiochemical purity of >99% and a specific activity of >3.7 GBq/ $\mu$ mole. To increase production yield at a later time, remote-controlled synthesis of non-carrier-added L-[1-<sup>11</sup>C]-tyrosine through a microwave-induced Bücherer-Strecker synthesis was developed.

### PET

Studies were performed on a whole-body tomograph that acquires 31 planes across an axial length of 10.8 cm. The measured resolution of the system is 6 mm FWHM transversally in the center of the field of view.

To prevent overlap of anatomical structures and head movements during the study, an individual foam-filled headmold was made. The method of fixation was standardized. The patient's head was positioned in the headmold so that the Frankfurter horizontal plane (defined as an imaginary line between the external ostium of the ear and the lower orbital rim) made a 110° angle with the horizontal bed position. This position was reached by requesting the patient to stretch the neck by moving the head backwards. For anatomical orientation, small radioactive markers were placed on the tip of the chin, the mandibular angles, the midline of the clavicles and the sternal notch.

Two transmission scans of 15 min each were obtained: one cranial and one caudal. The total distance was 21 cm. After transmission scanning, TYR (370 MBq) was injected

into a peripheral vein of the arm and the markers were placed. Data acquisition was started 20 min post injection. To cover the whole neck, 10-min cranial and caudal scans were made in reverse order as compared to the transmission scans.

Any visually positive hot spot on each emission scan was considered to be a metastatic hot spot. This procedure was identical to the FDG procedure published earlier (4), but left and right symmetrically located hot spots in the sagittal planes were assumed to be the salivary glands. Standardized uptake values were not calculated due to the poor results in the FDG study.

**Table 1.** The assessment of lymph node metastases of squamous cell carcinomas of the oral cavity

Patient Nr(sex,age)	Tumor Stage, location ‡ R / L	Metastases *					Neck Treatment †
		Clinical R / L	PET R / L	MRI R / L	CT R / L	Hist R / L	R / L
1 (m,73)	T2N0, floor mouth R	- / -	++ / ++	- / -		++ / -	SOND / -
2 (f,70)	T4N1, retromol.trig. R	+ / -	++ / -	++ / -		- / -	MRND / -
3 (m,53)	T4N2, floor mouth RL	++ / ++	++ / ++		++ / ++	++ / ++	MRND / MRND
4 (f,73)	T4N0, lower gum R	- / -	+ / +	- / +		- / -	SOND / SOND
5 (m,59)	T1N0, floor mouth L	- / -	- / -	- / -		- / -	- / SOND
6 (m,66)	T4N2a, floor mouth R	++ / -	++ / -	++ / -		++ / -	MRND / -
7 (f,69)	T2N0, oral cheek L	- / -	- / -		- / -	- / -	- / MRND
8 (m,64)	T4N2b, floor mouth R	++ / -	- / -		++ / -	- / -	MRND / -
9 (f,56)	T4N2b, floor mouth R	++ / -	++ / +		- / -	++ / -	SOND / SOND
10 (m,46)	T4N2b, floor mouth L	- / ++	- / ++	++ / ++		- / ++	- / MRND
11 (m,56)	T4N0, floor mouth L	- / -	- / -	- / +		- / ++	SOND / MRND

\* The clinical, PET, MRI, and histopathological staging of both sides of the neck (- = no suspicious nodes, + = one suspicious node, ++ = two or more suspicious nodes). † The neck treatment that has taken place (- = no treatment, SOND = supraomohyoid neck dissection, MRND = modified radical neck dissection). ‡ The T- and N- stage according to the UICC (1992) and AJCC (1988) classifications of the primary tumor and location. Retromol.trig. = retromolar trigone.



## MRI

Seven patients underwent MRI. T1-(TR = 650 msec, TE = 20 msec) and T2-(TR = 2000 msec, TE = 50-100 msec) weighted pulse sequences were obtained. A head coil was used to obtain axial and coronal slices with a slice thickness varying between 3-5 mm. We used the following radiologic criteria (2) to assess cervical metastases in patients with a primary SCC:

1. Nodes with a minimal axial diameter of 11 mm or more in the subdiaphragmatic region and 10 mm or more in the other lymph node-bearing regions were considered metastatic.
2. Groups of three or more lymph nodes of 9 or 10 mm in the subdiaphragmatic region and of 8 or 9 mm in the other lymph node drainage regions of the tumor were considered metastatic.
3. All nodes that showed irregular enhancement on MRI and were surrounded by a rim of enhancing viable tumor or lymph node tissue were considered metastatic.

## CT

Four patients underwent CT instead of MRI. Axial and coronal slices were made with a slice thickness varying between 5 - 10 mm. Intravenous contrast medium was administered to all patients. The criteria for delineating a lymph node metastasis were the same as those used for MRI.

## Histopathology

Shortly after the PET, MRI or CT studies, radical surgery of the primary tumor and selective or modified radical neck dissection was performed (median time interval between the studies and the surgical procedure was 4,5 days). The removed specimen was stretched out on a polystyrene pad and the coordinates were marked immediately after removal by the surgeon using colored pins. From the specimen, all lymph nodes were studied individually using H&E staining. From each lymph node, the largest diameter was measured for lymph nodes with a diameter of 2 cm or more, several samples were examined.

## Data Analysis

Applying standard manufacturer software, the transversal PET images were individually reoriented to sagittal and coronal planes to obtain a better view of the lymph nodes, especially of those lying in clusters. The images were analyzed visually by two observers

at the same time. Disagreements were solved by consensus. The number and location of the positive nodes were assessed.

A similar approach was done for the MRI and CT. The PET, MRI and CT observers were unaware of each other's results and of the histopathology. Sensitivity, specificity, positive and negative predictive values and accuracy were calculated for the lymph node metastases detected by PET, MRI and CT against histopathology. Finally, the TYR-PET results were compared with those obtained from an earlier FDG-PET study (4).

**Results**

Histopathology of the resected neck specimens depicted a total of 287 lymph nodes, 24 of which were metastatic. PET depicted 32 positive lymph nodes (Fig.1). Twenty of the 24 histopathologic metastatic lymph nodes were visualized with PET. The 12 other lymph nodes that showed positive with PET were normal on histopathological examination (Table 2). The smallest metastatic lymph node detected was 0.5 cm. Four metastatic lymph nodes were not detected with TYR-PET (0.4-1.2 cm).

MRI depicted 155 lymph nodes, 11 of which were positive lymph nodes. When compared with the histopathological results, five nodes were metastatic and six lymph nodes were normal. In the resected specimens, 15 metastatic lymph nodes were found after histopathological examination. Obviously, MRI missed 10 metastatic lymph nodes, which were between 0.5 - 1.5 cm (Table 2).

**Table 2.** The results of PET, MRI, CT and histopathology in the detection of lymph node metastases of squamous cell carcinomas of the oral cavity.

	Histopathology		
	metastatic	normal	total
PET positive	20	12	32
PET negative	4	251	255
total	24	263	287
MRI positive	5	6	11
MRI negative	10	134	144
total	15	140	155
CT positive	5	10	15
CT negative	4	113	117
total	9	123	132

Finally, for CT (132 lymph nodes were evaluated), of the nine histologically proven metastatic nodes, CT detected five. Ten lymph nodes that were positive on CT were normal on histopathological examination (Table 2). The metastatic lymph nodes missed by CT varied in size from 0.8 to 3.0 cm. The smallest metastatic lymph node detected with MRI or CT was 1.0 cm.

Sensitivity, specificity, positive and negative predictive values and accuracy were calculated for all three diagnostic imaging modalities (Table 3).

**Table 3.** Sensitivity, specificity, accuracy and predictive value of a positive and negative test (PVP, PVN) for PET-TYR, MRI, CT and PET-FDG\*.

\* results of study published earlier (4).

	PET TYR	MRI	CT	PET FDG*
sensitivity	83%	33%	55%	91%
specificity	95%	96%	91%	88%
accuracy	95%	90%	89%	88%
PVP	63%	45%	33%	48%
PVN	98%	93%	97%	99%

## Discussion

The presence of cervical lymph node metastases in SCC of the oral cavity will often change the extent of surgical treatment. For instance, at our institution a T1N0 oral cavity SCC is treated with local resection of the tumor alone and a "watchful waiting policy" is used for the neck. If metastatic lymph nodes are found, the treatment consists of resection of the primary tumor and a supraomohyoid or modified radical neck dissection. In case the primary tumor is stage T2 or more and no cervical lymph nodes are clinically evident (or evident by imaging), elective neck dissection is indicated. Thus, a reliable estimation of the presence of metastatic lymph nodes is needed to prevent over-treatment.

So far, the surgeon largely depends on palpation to assess the presence of metastatic lymph nodes. Several clinicians have sought more modern techniques that will allow better assessment of the presence of cervical metastatic lymph nodes. Van den Berkel et al. (12) described the assessment of lymph node metastasis in the neck with different

imaging modalities. They concluded that CT and MRI are superior to palpation in detecting or excluding metastatic neck disease. They also concluded that although it is possible to reliably upstage more than half of the clinically negative necks with CT, MRI and US, US-guided fine needle aspiration cytology (FNAC) is the most sensitive, specific and accurate technique to detect or exclude the presence of metastases preoperatively. However, with US-guided FNAC, no standardized permanent document is obtained and the accuracy of the technique fully depends on the examiner. Finally, Van den Brekel et al. concluded that patients with undoubtedly palpatory evidence of unilateral mobile metastases on the side of the primary tumor well confined to one side, or patients with bilateral palpatory mobile metastases, do not need US-guided FNAC. Also patients who need radiologic staging (CT or MRI) for their primary tumor need no US-guided FNAC of the neck, if the neck is included in the imaging. The reliability of CT and MRI, however, is doubtful and largely depends on the experience of the investigator.

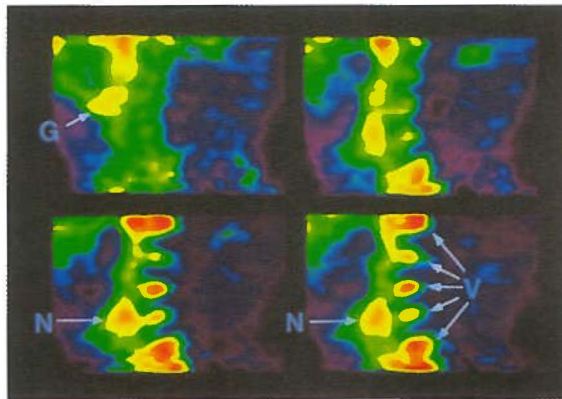


**Figure 1.** Example of sagittally reoriented PET images of a metastatic lymph node in the jugulum (N) of a patient with a  $T_2N_1$  carcinoma of the oral cavity. There is also high uptake in the submandibular gland (G) and in the bone marrow of the cervical vertebrae (V).

We have explored the possibilities of PET for the detection of metastatic lymph nodes. The main advantage of PET over the other imaging techniques is that it evaluates metabolism rather than structure. In an earlier investigation, we studied the possibilities of the widely used tracer FDG (4).

Our previous results showed that PET-FDG is a good indicator of the presence of

metastatic lymph nodes. However, several false-positive results were encountered due to the fact that reactive lymph nodes also yield a positive signal. Even with the standardized uptake values of the true-positive and false-positive lymph nodes, no differentiation could be made. Indeed, Kubota et al. (3) have shown that leukocytes also have high glucose consumption and consequently high FDG uptake. A main quest for PET research still is to find a way to differentiate between cancerous cells and inflammatory cells.

To circumvent this problem, we studied the possibilities of TYR as a tracer. This tracer shows high incorporation rates into proteins while, when catabolized, the  $^{11}\text{C}$ -label leaves the body as  $^{11}\text{CO}_2$  in an earlier step. Our experiences with TYR in other types of cancer are promising (9,11). TYR-PET compared favorably with CT and MRI in terms of sensitivity, accuracy and positive predictive values. Compared with the FDG results from our previous paper (4), TYR has higher specificity, accuracy and positive predictive values. Therefore, we believe that TYR-PET appears to be the most reliable technique so far to assess the presence of metastatic lymph nodes in the necks of patients with SCC of the oral cavity.

Despite these favorable results, there were more false-negatives ( $n=4$ ) than in our earlier FDG study. One metastatic lymph node was in a cluster of five interconnected metastatic lymph nodes. Another metastatic lymph node was in close proximity to the primary tumor and the submandibular gland. Despite its size of 1.2 cm, this metastasis was not detected. The remaining two undetected metastatic lymph nodes were 0.4 cm in size (Table 2).

The fact that one metastatic lymph node in a cluster of five interconnected metastases was not found, is probably due to the high uptake of TYR from the neighboring positive lymph nodes and the partial volume effect. Another explanation could be that no delineation is possible from that cluster of metastatic lymph nodes due to the camera resolution used. However, this negative PET result did not affect the clinical management of the patient.

Similarly, one metastatic lymph node was not visualized because of the high activity from the primary tumor and the submandibular gland, which were closely related to each other. The active uptake of TYR by the salivary glands may be a severe drawback of the TYR-PET technique.

Finally, TYR-PET did not detect two small (0.4 cm) metastatic lymph nodes. The size of these metastatic nodes suggests that size is a factor in undetected nodes. Indeed, 0.4 cm is at the lower end of the resolution of current PET cameras. Newer systems have a slightly better resolution, but there is a physical limitation of about 0.3 cm. Consequently, PET will never be suitable for detecting microscopic disease, although much smaller metastatic lymph nodes can be better identified than with MRI or CT. It can also be argued that the metastatic lymph nodes could not be delineated from the surrounding tissue because of a low protein synthesis rate. Minn et al. (14), in their

study of a specially collimated gamma camera and FDG, suggested that low glycolytic activity could be the explanation for undetected metastases of a breast tumor. An extrapolation of this suggestion could explain that it is also possible to have a low protein synthesis rate.

The smallest lymph node detected by TYR-PET was 0.5 cm, whereas the smallest detected metastatic lymph node with MRI and CT was 1.0 cm. This latter finding should be attributed to the radiologic criteria used. Van den Brekel et al. (2) consider 9-10 mm in the subdiaphragic region and 10-11 mm in the other lymph node drainage regions as the critical size to differentiate between metastases or reactive lymph nodes. Consequently, specificity of this technique is increased at the cost of lower sensitivity, since smaller lymph nodes are excluded by definition.

The number of false-positive lymph nodes with TYR-PET was relatively high: 12 lymph nodes. The origin of the positive signal is yet unclear, since all nodes were normal on histological examination. There were no reactive changes in these false-positive lymph nodes. Leskinen-Kallio et al. (15) reported on the uptake of amino acids in inflammatory processes. They found that MET accumulated slightly in a breast abscess (15). Lindholm et al. (6) also described the uptake of MET in inflammatory processes. FDG uptake in inflammatory tissues has been reported by other authors. Although histology gave no evidence of inflammatory processes yielding a positive signal, we have to realize that the advantage of  $^{11}\text{C}$ -labeled amino acids over FDG is probably not a principal difference because it is derived from a small population of patients. A larger patient population should be studied to confirm this.

In all patients we found that TYR accumulates markedly in the sublingual, submandibular and/or parotid glands and sometimes in bone marrow. This high uptake in the salivary glands impairs the analysis of PET images, especially when the primary tumor or metastases are localized close to these structures. The submandibular lymph nodes are one of the first nodal echelons which will be infested with micrometastases and are therefore difficult to detect. Lindholm et al. (6) described this phenomenon with MET, but they mentioned that these hot salivary glands could be landmarks to make it easier to localize the primary tumor in a PET image. We believe that placement of markers on earlier defined structures is preferable to landmarks in the field of view.

For clinical PET studies, FDG and TYR are two reliable tracers suitable for the detection of lymph node metastasis of SCC of the oral cavity. The higher sensitivity and predictive value of a negative test is an advantage of FDG-PET over TYR-PET. The relatively high uptake in reactive tissue, however, is a severe drawback of FDG. The specificity, accuracy and positive predictive value make TYR-PET more favorable, although the TYR uptake in the salivary glands impairs image analysis.

Consequently, we slightly prefer FDG-PET in patients with clinically negative neck

metastases. Patients with palpable lymph nodes in the neck should be scanned with TYR-PET.

PET imaging, as applied in this and the previous study, is rather cumbersome for the patient. It is time-consuming and requires that the patient lie quietly for a long time. Most of the time is needed to obtain two transmission scans (total time 1 hr), and, including the emission scans, the procedure takes more than 1.5 hr. To reduce this time frame, a less time-consuming, technique is needed. A few years ago, Guerrero et al. (16) and Dahlbom et al. (17) introduced whole-body scanning software for ECAT cameras (16,17). In this software, no transmission scanning is applied, and the scan time per bed position is often less than 10 min. We are currently investigating, whether whole-body scanning for the head and neck region yields results similar to those in this study

A metabolic imaging technique as TYR-PET is an important diagnostic tool in the assessment of the presence of metastatic lymph nodes in patients with SCC of the oral cavity. The technique is superior to imaging techniques based on structural alterations such as CT and MRI. The high specificity, accuracy and predictive values make TYR-PET suitable for further evaluation of neck metastases. The high sensitivity and negative predictive value makes FDG-PET preferable for evaluation of neck metastases with stage N<sub>0</sub>.

## References

1. Van den Brekel MWM, Castelijns JA, Croll GA, et al. Magnetic resonance imaging versus palpation of cervical lymph node metastases. *Arch Otolaryngol Head Neck Surg* 1991;117:666-673.
2. Van den Brekel MWM, Stel HV, Castelijns JA, et al. Cervical lymph node metastasis: assessment of radiologic criteria. *Radiology* 1990;177:379-384.
3. Warburg O. *The metabolism of tumors*. London: Arnold Constable; 1930:75-327.
4. Braams JW, Pruim J, Freling NJM, et al. Detection of lymph node metastases of squamous cell cancer of the head and neck with PET-FDG and MRI. *J Nucl Med* 1995;2:211-216.
5. Kubota R, Yamada S, Kubota K, Ishiwata K, Tamahashi N, Ido T. Intratumoral distribution of fluorine-18-fluorodeoxyglucose in vivo: high accumulation in macro-phages and granulation tissues studied by microautoradiography. *J Nucl Med* 1992;33:1972-1980.
6. Lindholm P, Leskinen-Kallio S, Minn H, et al. Comparison of fluorine-18-fluorodeoxyglucose and carbon-11-methionine in head and neck cancer. *J Nucl Med* 1993;34:1711-1716.
7. Ishiwata K, Kubota K, Murakami M, et al. Re-evaluation of amino acid-pet studies: can the protein synthesis rates in the brain and tumor tissues be measured in vivo? *J Nucl Med* 1993;34:1936-1943.
8. Daemen BJG, Elsinga PH, Paans AMJ, Wieringa AR, Konings AWT, Vaalburg W. Radiation-induced inhibition of tumor growth as monitored by PET using L-1-[<sup>11</sup>C]-tyrosine and <sup>18</sup>F-fluoride-oxyglucose. *J Nucl Med* 1992;33:373-379.
9. Daemen BJG, Zwertbroek R, Elsinga PH, Paans AMJ, Doorenbos H, Vaalburg W. PET studies with L-1-[<sup>11</sup>C]-tyrosine, L-[methyl-<sup>11</sup>C]methionine and <sup>18</sup>FDG in prolactinomas in relation to bromocryptine treatment. *Eur J Nucl Med* 1991;18:453-460.
10. Shanmugaratnam K, Sobin LH. *Histological typing of upper respiratory tract tumors*. Geneva: World Health Organization, 1978.
11. Bolster JM, Vaalburg W, Paans A, et al. Carbon-11 labeled tyrosine to study tumor metabolism by positron emission tomography (PET). *Eur J Nucl Med* 1986;12:321-324.
12. Van den Brekel MWM. *Assessment of lymph node metastases in the neck*. Thesis Free University Amsterdam, Utrecht: Elinkwijk 1992.
13. Kubota R, Yamada S, Kubota K, Ishiwata K, Ido T. Microautoradiographic study of <sup>18</sup>F-FDG: high accumulation in granulation tissues and phagocytes in mouse tumor tissue in vivo. *J Nucl Med* 1992;33:840-841.
14. Minn H, Soini I. Fluorine-18-fluorodeoxyglucose scintigraphy in diagnosis and follow-up of treatment in advanced breast cancer. *Eur J Nucl Med* 1989;15:61-66.
15. Leskinen-Kallio S, Nägren K, Lehtikoinen P, Ruotsalainen U, Joensuu H. Uptake of <sup>11</sup>C-methionine in breast cancer studied by PET: an association with the size of S-phase fraction. *Br J Cancer* 1991;64:1121-1124.
16. Guerrero TM, Hoffman EJ, Dahlbom M, Cutler PD, Hawkins RA, Phelps ME. Characterization of a whole-body imaging technique for PET. *IEEE Trans Nucl Sci* 1990;37:676-680.
17. Dahlbom M, Hoffman EJ, Hoh CK, et al. Whole-body positron emission tomography: part 1. Methods and performance characteristics. *J Nucl Med* 1992;33:1191-1199.



- CHAPTER 5 -

**DETECTION OF METASTATIC LYMPH NODES IN THE NECK WITH  
PET-TYROSINE IN WHOLE BODY MODE**

**Jan Willem Braams, Jan Pruim, Peter G.J. Nikkels,  
Willem Vaalburg, Albert Vermey and Jan L.N. Roodenburg.**

Departments of:    Oral and Maxillofacial Surgery  
                         Pathology  
                         PET Center  
                         Surgical Oncology

**Groningen University Hospital, Groningen, The Netherlands**

Submitted Cancer

To detect metastases the uptake of L-[1-<sup>11</sup>C]-tyrosine (TYR) in cervical lymph nodes of twenty-two patients with squamous cell carcinoma (SCC) of the oral cavity was studied with Positron Emission Tomography (PET) in the whole body mode (PET-TYRWB). This study was not corrected for attenuation. The benefit of the WB-technique is the short investigation time compared with the normal scanning procedures. **Methods.** The PET-TYRWB results were compared with clinical and histopathologic findings and with previous data of patients studied with PET-TYR. This data was attenuation corrected. Sensitivity, specificity, accuracy and the positive and negative predictive values were calculated. **Results.** PET-TYRWB had a sensitivity of 90% and a specificity of 99%. The sensitivity and specificity of PET-TYR were 83% and 95%, respectively. **Conclusions.** Neck node metastases of SCC's of the oral cavity can well be visualized with PET-TYRWB. The results were comparable with the previous PET-TYR results. The reduced camera-time makes this investigation more convenient for the patient.

## Introduction

Staging of cervical lymph nodes in patients with squamous cell carcinomas (SCC) of the head and neck is one of the keystones in treatment planning. Staging of neck nodes by palpation yields false-negative results in 0% to 77% of cases (1,2), depending on the site (3), size (4) and other parameters (5) of the primary tumor.

To date, computer tomography (CT) and magnetic resonance imaging (MRI) have enabled detection of lymph node metastases (6-8). Unfortunately these modalities have not led to a more conservative approach towards treatment of the neck in most institutions. Consequently the need for a more sensitive technique remains.

An alternative way of cancer imaging is to visualize metabolic characteristics of tumor cells. Malignant cells have increased glucose consumption due to an increased glycolysis (9). Various investigators have therefore applied 2-deoxy-2-[<sup>18</sup>F]fluoro-D-glucose (FDG) as a marker of tumor tissue in imaging with Positron Emission Tomography (PET). In SCC of the oral cavity, PET-FDG is able to detect nodal metastases in the neck (10-12). However, PET-FDG is hampered by a high false positive rate due to accumulation of FDG in inflammatory tissues (10,13).

As an alternative <sup>11</sup>C-labeled amino acids, e.g. methyl-labeled <sup>11</sup>C-methionine, have been evaluated. Lindholm et al. found that L-[methyl-<sup>11</sup>C]methionine (MET) is useful for PET imaging of primary head and neck cancer and cervical metastases (14).

For this purpose we have studied the carboxyl-labelled amino acid tyrosine, L-[<sup>11</sup>C]tyrosine (TYR) as radiopharmaceutical, because TYR reflects the protein synthesis rate (PSR) in cancer cells (15). So far, TYR has been successfully used in rats and humans to visualize different types of tumors and to quantitate the PSR (14-16). Braams et al. studied the use of TYR in patients with head and neck cancer and concluded that with the use of TYR, metastases of SCC's of the oral cavity can be visualized with high sensitivity and specificity (17). With the introduction of PET in combination with FDG or TYR, the sensitivity and specificity of the assessment of the presence of small non-palpable cervical lymph node metastases (0.5 -1.0 cm) of SCC has improved considerably as compared to MRI and CT (10-12,17).

However, PET-imaging in the previous studies is time consuming and requires the patient to lie still for a long time. Most of the time is needed to obtain transmission scans (total time 1 hour) in order to correct for attenuation. Including the emission scans, the total procedure takes more than 1.5 hours. A less time consuming technique is needed. Guerrero et al. (18) and Dahlbom et al. (19) introduced whole body scanning software for ECAT cameras. In such a study, no transmission scan is performed, and the scan time per bed position is often less than 10 min. In this study we have investigated whether PET-TYRWB (non-attenuation corrected) for neck node metastases yields similar results to those in our previous PET-TYR study (17).

### Materials and Methods

#### Patients

Twenty-two patients were submitted to the Departments of Maxillofacial Surgery and Surgery/Oncology of the Groningen University Hospital the Netherlands for treatment of a SCC of the oral cavity. These patients (nineteen males (mean age 50.9 yrs) and three females (mean age 58 yrs)) with histologically verified primary SCC of the mucosa of the oral cavity and a staging of the neck N0 - N2b were studied. (table 1).

Staging of the tumor and its metastases was based on the TNM-classification of the - International Union against Cancer (UICC, 1992) and American Joint Committee on Cancer (AJC, 1989). The median time interval between the PET-study and the surgical procedures was 3.5 days (range 1-5 days). Histological typing of the primary tumor and metastases was performed according to the WHO (1978) classification (20). After clinical examination a therapeutic or elective neck dissection was indicated in all patients. Patient characteristics are presented in table 1. None of the patients received preoperative radiotherapy or chemotherapy. The study was approved by the Medical Ethics Committee of the Groningen University Hospital. A written informed consent was obtained. Patient characteristics of the previous studied 11 PET-TYR patients studied were published earlier (17).

#### PET imaging

The camera used was a Siemens ECAT 951/31 whole body machine (Siemens CTI, Knoxville, USA). The device acquires 31 planes across an axial length of 10.8 cm. The measured resolution of the system is 6 mm full width at half maximum (FWHM) transversally in the center of the field of view. For reconstruction of the images a Hanning filter was used.

The patients were fasted overnight before the PET study. The non-attenuation corrected whole body scans were made 30 minutes after administration of 370 MBq of TYR into a peripheral vein of one of the upper extremities. To cover the head and neck area 5 bed positions of 3 minutes each were scanned. Images were visually assessed using standard ECAT software. Depending on the location every positive hot spot on the images was considered to be the primary tumor or a metastasis. Left and right symmetrically located hot spots in the sagittal planes were assumed to be the salivary glands.

L-[1-<sup>11</sup>C]-tyrosine was produced by a remote controlled synthesis of a non-carrier added method via a microwave induced Bücherer-Strecker synthesis, as described previously (17).

DETECTION OF METASTASES WITH PET-TYR IN WHOLE BODY MODE

**Table 1.** Assessment of lymph Node Metastases of SCCs of the Oral cavity

patient no.	sex	Age (yrs)	tumor		metastases*			neck treatment†
			Stage, location R/L	Clinical R/L	PET R/L	CT R/L	Hist. R/L	R/L
1	M	47	T4N1,retromol.trig R	+/-	+/-		+/-	SOND/-
2	M	56	T4N0,floor mouth L	-/-	-/++		-/++	SOND/MRND
3	M	47	R1,floor mouth L	-/-	++/++		-/++	SOND/SOND
4	M	60	T2N0,lower gum L	-/-	-/-		-/-	-/SOND
5	M	47	T4N0,floor mouth R	-/-	-/-		-/-	SOND/SOND
6	M	50	T4N1,oropharynx R	+/-	++/-		++/-	MRND/-
7	M	49	T4N2,floor mouth RL	++/++	++/++	++/++	++/++	MRND/MRND
8	V	46	T2N1,tongue R	+/-	+/-	+/-	+/-	MRND/-
9	M	69	T4N0,lower gum R	-/-	++/-	++/-	++/-	MRND/-
10	V	63	T1N0,floor mouth R	-/-	-/-		-/-	SOND/-
11	M	53	T4N0,lower gum L	-/-	-/-	-/++	-/-	-/SOND
12	M	70	T2N0,floor mouth R	-/-	-/-		-/-	SOND/-
13	M	60	T4N2,floor mouth RL	+/-	+/-	+/+	+/-	SOND/-
14	M	59	T1N1,tongue L	-/+	-/-	-/++	-/+	-/MRND
15	M	51	T4N0,floor mouth L	-/-	-/+	-/++	-/+	-/MRND
16	M	65	T1N1,lip R	+/-	++/-		++/-	MRND/-
17	M	63	T3N0,tongue R	-/-	-/-		-/-	SOND/-
18	M	38	T4N2b,floor mouth R	++/-	++/-	++/-	++/-	MRND/-
19	V	66	T4N0,floor mouth	-/-	-/-	-/-	-/-	SOND/SOND
20	M	26	T3N0,tongue L	-/-	-/-		-/-	-/MRND
21	M	67	T2N0,floor mouth L	-/-	-/++		-/-	-/SOND
22	M	34	T1N0,floor mouth L	-/-	-/-		-/-	-/SOND

\* The clinical, PET, MRI, and histopathological staging of both sides of the neck (- = no suspicious nodes, + = one suspicious node, ++ = two or more suspicious nodes). † The neck treatment that has taken place (- = no treatment, SOND = supraomohyoid neck dissection, MRND = modified radical neck dissection). ‡ The T- and N- stage according to the UICC (1992) and AJCC (1988) classifications of the primary tumor and location. Retromol.trig. = retromolar trigone.

### CT imaging

In nine patients a CT was performed with a Philips Tomoscan SR (Philips, Eindhoven, The Netherlands). Axial and coronal slices were made with a slice thickness varying between 5-10 mm. In all patients intravenous contrast medium (Telebrix<sup>®</sup> 350) was administered. The CT scanning was only performed in patients if there was an indication in the clinical protocol.

The following radiologic criteria (22) for assessing cervical metastases in patients with a primary squamous cell carcinoma were used:

1. Nodes with a minimal axial diameter of 11 mm or more in the subdiaphragic region and 10 mm or more in the other lymph node-bearing regions were considered metastatic.
2. Groups of three or more lymph nodes of 9 or 10 mm in the subdiaphragic region and of 8 or 9 mm in the other lymph node drainage regions of the tumor were considered metastatic.
3. All nodes that showed irregular enhancement on MRI and were surrounded by a rim of enhancing viable tumor or lymph node tissue were considered metastatic.

### Histopathology

Radical surgery of the primary tumor and a selective or modified radical neck dissection was performed after a median time interval of 3.5 days with the PET study. The removed specimen was stretched out on a polystyrene pad and the coordinates were marked immediately after removal by the surgeon using colored pins. From the specimen all lymph nodes were studied on an individual basis, using haematoxylin-eosin staining. From each lymph node the largest diameter was measured. From lymph nodes with a diameter of 2 cm or more several samples were examined. The histopathology was done by one pathologist who was unaware of the PET-results

### Data analysis

Applying standard CTI/ECAT software, PET-images were analysed visually by one observer. The number and location of the positive nodes were assessed. Using histopathology as gold standard, sensitivity, specificity, accuracy, predictive value for a positive and negative test were calculated for the lymph node metastases detected by PET. Finally, the PET-TYRWB results were compared with those obtained earlier with PET-TYR (17).

## Results

Histopathology of the resected neck specimens showed a total of 579 lymph nodes of which 39 had metastatic disease. Thirty-five of the 39 metastatic lymph nodes were visualized with PET. In addition, six other lymph nodes were visualized with PET, but proved to be normal on histopathological examination (table 2). The smallest metastatic lymph node detected was 6 mm. The size of the six metastatic lymph nodes which were not detected with PET-TYR ranged from 4 to 7 mm.

**Table 2.** PET, CT and Histopathology Results.

Modality	Histopathology		
	Metastatic	Normal	Total
PET positive	35	6	41
PET negative	4	534	538
Total	39	540	579
CT positive	24	6	30
CT negative	5	190	195
Total	29	196	225

Sensitivity, specificity, accuracy, predictive value for a positive and negative test were calculated and are summarized in table 3.

A phenomenon that was observed in this study was the accumulation of TYR in the major salivary glands (parotid, submandibular and sublingual glands).

In nine patients CT was performed. Histopathology showed 29 positive nodes of a total of 225 lymph nodes. CT detected 24 of the 29 histologically proven metastatic lymph nodes. In addition, six nodes that were positive on CT were normal on histopathological examination (table 2). The metastatic lymph nodes that were missed by CT varied in size from 6 to 15 mm. The smallest metastatic lymph node detected with CT was 10 mm.

**Table 3.** Sensitivity, Specificity, Accuracy, Positive Predictive Value (PPV) and Negative Predictive value (NPV) for PET-TYRWB, PET-TYR\*.  
\*Results of previously published study (17).

	PET-TYRWB n = 22	PET-TYR* n = 11
Sensitivity(%)	90	83
Specificity(%)	99	95
Accuracy(%)	98	95
PPV(%)	85	63
NPV(%)	99	98

## Discussion

The presence of cervical lymph node metastases in SCC of the oral cavity will determine the treatment. Thus, a reliable estimation of the presence of the metastatic lymph nodes in cases of SCC of the oral cavity and oropharynx is needed to prevent over or undertreatment.

So far, imaging techniques like CT, MRI and ultrasound (US) gave better results in detecting cervical lymph nodes as compared to palpation (23). The specificity of US was improved by combining this technique with fine needle aspiration biopsies for cytological evaluation. The authors report a sensitivity of 90% and a specificity of 100%. In a multicenter trial US-guided fine needle aspiration cytology (USgFNAC) was compared with CT in detecting lymph node metastasis in the clinically negative neck (24). In sixty-four neck sides a sensitivity of USgFNAC was reported of 48% and a specificity of 100%. The main problems with USgFNAC are that there is no standardized permanent document obtained and the accuracy of the technique fully depends on the experience of the examiner.

With the introduction of PET, several institutions studied the head and neck area (10,11,14). Our previous studies showed that FDG and TYR are reliable tracers for the detection of lymph node metastases (10,17). However, several false positive FDG results were encountered (10). To circumvent this problem, we studied TYR as a tracer. TYR has a higher specificity, accuracy and positive predictive values as compared with PET-FDG (17). The PET-TYRWB results are better than the results from our previous PET-TYR study (17). These better results were not expected, since WB images were not corrected for attenuation. In comparison with PET-TYR, PET-TYRWB appeared to be



reliable and more convenient.

Another benefit of PET is that smaller metastatic lymph nodes of at least 6 mm can be detected. The radiologic criteria of CT and MRI exclude lymph nodes smaller than 9 mm. In case enlarged nodes are visualized with US the optimal size criteria for a palpatory negative neck is 8 mm for the subdigastric nodes and 7 mm elsewhere in the neck. For the palpatory positive nodes the size criteria is between the 9 and 10 mm. For aspiration cytology, the minimal axial diameter of these lymph nodes must be 4-5 mm.

Despite the favourable PET-TYRWB results 4 dissected lymph nodes were false negative. Two metastatic lymph nodes were in close proximity of a salivary gland. Another metastatic lymph node was 5 mm in diameter and one lymph node was interconnected in a cluster of several lymph nodes. It can be argued that due to the high uptake of the salivary glands, metastatic lymph nodes cannot be delineated, which are lying in close proximity of these glands.

The uptake of TYR in sublingual, submandibular and parotid glands is still a problem that impairs the analysis of the PET images, especially when the primary tumor or the metastases are located close to these structures. An explanation for the high TYR uptake by salivary glands is the high secretory activity of these glands. In a pilot animal experiment we observed that pretreatment with atropine (to reduce the salivary secretion) reduces the TYR uptake in rat major salivary glands. This may be a solution for the clinical problem.

Similarly, the metastatic lymph node which was interconnected with other metastatic lymph nodes with a high uptake was not visualized with PET-TYRWB. However, the clinical management of the patient was not affected due to the metastatic node missed by PET-TYRWB.

PET-TYRWB did not detect a small metastatic lymph node of 5 mm due to the resolution of the camera. The size of this metastatic lymph node suggests that size is a factor in undetected nodes, as previously concluded (10,17).

In this study we found 6 false positive nodes. Histopathology showed that in these nodes there were no reactive changes, so the origin of the signal is yet unclear. May be the relatively long interval between the PET investigation and the neckdissection can explain the loss of reactive changes

The PET-TYRWB results have a slight benefit over the CT results. However, it can be discussed that the small number of patients impaired the validity of the data for CT. Only a few studies were performed to compare the efficacy of different radiologic modalities. The largest study was performed by van den Brekel, et al. (23) The results of this study were that CT examination showed a sensitivity of 83% which was higher than for palpation (67%) and US (75%) and comparable to the sensitivity of MRI (82%). However, the specificity of CT was rather low in all groups of patients: 70% for all sides, 47% for the palpatory positive nodes and 78% for palpable negative sides. The

MRI-results were respectively 81%, 63% and 88% (23). The CT results of the multicenter trail reported by Takes, et al. (24) demonstrated a sensitivity of 54%, and a specificity of 92%.

The main advantage of PET above CT, MRI and US according to the literature is the higher sensitivity and the possibility of PET to visualize smaller metastatic lymph nodes (6-9 mm). Since, the extent of the neck dissection is determined by the spread of the metastatic disease. It can also be argued that due to the radiologic size-criteria of 9 mm used for CT and MRI the specificity is increased but at the cost of lowering the sensitivity, since smaller nodes with no irregular enhancement are excluded by definition.

This study suggests that comparable results can be obtained with PET-TYRWB as with PET-TYR. The advantage of the whole body mode without attenuation correction is the reduced camera-time resulting in a more convenient procedure for the patient, and a possibility to use the PET more cost effective.

In conclusion, PET-TYRWB (non-attenuation corrected) is a good method for the detection of cervical lymph node metastases of SCC of the oral cavity. In contrast with CT, MRI and US lesions of 6-9 mm can be detected. Application of USgFNAC is hampered by the experience of the examiner and that no permanent document is obtained. The results of PET-TYRWB are comparable with the results of PET-TYR. PET-TYRWB requires a shorter scanning time than PET-TYR and is therefore less cumbersome for the patient and more cost effective. So we can conclude that the non-attenuation corrected PET-TYRWB is preferable above attenuation corrected PET-TYR.

---

**References**

1. Spiro RH, Strong EW. Epidermoid carcinoma of the mobile tongue: treatment by partial glossectomy alone. *Am J Surg* 1971;122:707-710.
2. McGraven MH, Bauer WC, Ogura JH. The incidence of cervical lymph node metastasis from epidermoid carcinoma of the larynx and their relationship to certain characteristics of the primary tumor. *Cancer* 1961;14:55-66.
3. Ali S, Tiwari RM, Snow GB. False positive and false negative neck nodes. *Head Neck Surg* 1985;8:78-82.
4. Byers RM, Wolf PF, Ballantyne AJ. Rationale for elective modified neck dissection. *Head Neck Surg* 1988;10:160-167.
5. Okamoto M, Ozeki S, Watanabe T, Iida Y, Tashiro H. Cervical lymph node metastasis in carcinoma of the tongue. Correlation between clinical and histopathological findings and metastasis. *J Cranio Max Fac Surg* 1988;16:31-34.
6. Van den Brekel MWM, Castelijns JA, Croll GA, et al. Magnetic resonance imaging vs palpation of cervical lymph node metastasis. *Arch Otolaryngol Head Neck Surg* 1991;117:666-673.
7. Stern WBR, Silver CE, Zeifer BA, Persky MS, Heller KS. Computed tomography of the clinically negative neck. *Head Neck* 1990;12:109-113.
8. Close LG, Merkel M, Vuitch MF, Reisch J, Scheafer SD. Computed tomographic evaluation of regional lymph node involvement in cancer of the oral cavity and oropharynx. *Head Neck* 1989;11:309-317.
9. Warburg O. *The metabolism of tumors*. London: Arnold Constable 1930;75-327.
10. Braams JW, Pruijm J, Freling NJM, et al. Detection of lymph node metastases of squamous cell cancer of the head and neck with PET-FDG and MRI. *J Nucl Med* 1995;2:211-216
11. Jabour BA, Choi Y, Hoh CK, et al. Extracranial head and neck: PET imaging with 2-[F-18]Fluoro-2-Deoxy-D-glucose and MR Imaging correlation. *Radiology* 1993;186:27-35
12. Conti PS, Lilien DL, Hawley K, et al. PET and [<sup>18</sup>F]-FDG in Oncology: A Clinical Update. *Nucl Med Biol* 1996;23:717-735
13. Kubota R, Yamada S, Kubota K, Ishiwata K, Tamahashi N, Ido T. Intratumoral distribution of fluorine-18-fluorodeoxyglucose in vivo: High accumulation in macrophages and granulation tissues studied by microautoradiography. *J Nucl Med* 1992;33:1972-1980.
14. Lindholm P, Leskinen-Kallio S, Minn H, et al. Comparison of fluorine-18-fluorodeoxyglucose and carbon-11-methionine in head and neck cancer. *J Nucl Med* 1993;34:1711-1716.
15. Ishiwata K, Kubota K, Murakami M, et al. Re-evaluation of amino acid-PET studies: can the protein synthesis rates in the brain and tumor tissues be measured in vivo. *J Nucl Med* 1993;34:1936-1943.
16. Willemsen ATM, van Waarden A, Paans AMJ, et al. In vivo protein synthesis rate determination in primary or recurrent brain tumors using L-[1-<sup>11</sup>C]-Tyrosine and PET. *J Nucl Med* 1995;36:411-419.
17. Braams JW, Pruijm J, Nikkels PGJ, Roodenburg JLN, Vaalburg W, Vermey A. Nodal spread of squamous cell carcinoma of the oral cavity detected with PET-tyrosine, MRI and CT. *J Nucl Med* 1996;37:897-901.
18. Guerrero TM, Hoffman EJ, Dahlbom M, Cutler PD, Hawkins RA, Phelps ME. Characterization of a whole body imaging technique for PET. *IEEE Transact Nucl Sci* 1990;37:676-680.

19. Dahlbom M, Hoffman EJ, Hoh CK, Schiepers C, Rosenqvist G, Hawkins RA, Phelps ME. Whole-body positron emission tomography: Part 1. methods and performance characteristics. *J Nucl Med* 1992;33:1191-1199.
20. Shanmugaratnam K, Sobin LH. Histological typing of upper respiratory tract tumors. Geneva: World Health Organization, 1978
21. Bolster JM, Vaalburg W, Paans A, et al. Carbon-11 labelled tyrosine to study tumor metabolism by positron emission tomography (PET). *Eur J Nucl Med* 1986;12:321-324.
22. Van den Brekel MWM, Stel HV, Castelijns JA, et al. Cervical lymph node metastasis: assessment of radiologic criteria. *Radiology* 1990;177:379-384.
23. Van den Brekel MWM, Castelijns JA, Stel HV, et al. Modern imaging techniques and ultrasound-guided aspiration cytology for the assessment of neck node metastases: a prospective comparative study. *Eur Arch Otorhinolaryngol* 1993;250:11-17.
24. Takes RP, Righi P, Meeuwis CA, Manni JJ, Knegt P, Baatenburg de Jong RJ, et al. The value of ultrasound with ultrasound-guided fine needle aspiration biopsy compared to computed tomography in the detection of regional metastases in the clinically negative neck. *Br J Cancer* 1998;77:16.

- CHAPTER 6 -

**DETECTION OF ORAL DYSPLASIA IN  
ANIMALS WITH FDG AND TYROSINE**

**Jan Willem Braams, Max J.H. Witjes, Corina A.A.M. Nooren, Peter G.J. Nikkels,  
Willem Vaalburg, Albert Vermey and Jan L.N. Roodenburg**

**Departments of:      Oral and Maxillofacial Surgery  
                                 Pathology  
                                 PET Center  
                                 Surgical Oncology**

**Groningen University Hospital, Groningen, The Netherlands**

**In press J Nucl Med**

The uptake of  $^{18}\text{F}$ -fluorodeoxyglucose (FDG) and L-[1- $^{11}\text{C}$ ]Tyrosine (TYR) was investigated in male Wistar albino rats with chemically induced dysplasia and oral squamous cell carcinoma (SCC) to correlate the uptake values with the grade of dysplasia.

**Methods:** The palate of 54 rats was painted three times a week with 4-nitroquinoline 1-oxide (4NQO) to create different stages of dysplasia and SCC. After 2,4,6,8,12,-16,20,26 and 30 weeks these rats were investigated with PET. Immediately thereafter the rats were sacrificed, and were histologically prepared. Standardized uptake values (SUV) were calculated of the palate of the rats and correlated with the Epithelial Atypia Index (EAI) and the thickness of the epithelial layer. **Results:** The SUV-TYR correlated with the EAI and the epithelial thickness, respectively 0.5 and 0.74. No correlation could be found for SUV-FDG vs EAI and the epithelial thickness. **Conclusion:** TYR showed higher uptake values for dysplasia and SCC than FDG. It appeared that for the detection of oral dysplasia the tissue hyperplasia is more important than malignant features of dysplastic mucosa.

## Introduction

Positron Emission Tomography (PET) is currently under investigation as a tool for the detection of cancer. PET can accurately monitor the metabolic route of certain radioactive labeled nutrients, receptor ligands, drugs and other radiolabeled compounds. In this technique the increased demand of tumor cells for certain nutrients is exploited to detect tumor tissue and to monitor therapy. Areas of high nutrient demand are displayed as areas with a high radioactive signal. The most widely used tracer is  $^{18}\text{F}$ -fluorodeoxyglucose (FDG) with which it is possible to monitor the increased glucose metabolism in cancer cells. Over the years, the application of FDG showed that this tracer is not optimal in all cases (1). A drawback of FDG for the detection of tumor tissue is the uptake in inflammatory tissues (2-4). Also in regions with a high basal metabolism FDG is not very suitable (5-8). Nevertheless, the sensitivity and specificity of PET-FDG to detect tumor tissue is often higher than that of CT, MRI or Spect.

Jabour et al.(9) studied the potential of FDG in the detection of primary tumors and metastases in the head and neck region. They concluded that non-enlarged lymph nodes, negative for metastatic disease according to MRI and CT, can be detected by PET-FDG. Braams, et al. (10) concluded that PET-FDG detects lymph node metastases with a high sensitivity (91%) and a somewhat lower specificity (88%). However, a substantial number of false positive lymph nodes are usually detected by PET-FDG. The positive predictive value of PET-FDG is somewhat less than 50%. Despite the impressive sensitivity, the results of the FDG studies show that there is need for more cancer specific tracers. Other metabolic processes were exploited, such as the rates of protein -, RNA - or DNA-synthesis (11,12). To visualize the protein synthesis rate (PSR), L-[1- $^{11}\text{C}$ ]-Tyrosine (TYR) was introduced (13). The results of PET-TYR in human studies are very promising in terms of sensitivity (83%) and specificity (95%) for the detection of several types of cancer (14). The positive predictive value of PET-TYR was approximately 63%. The high uptake of TYR in the salivary glands and bone marrow impaired the results because the high signal from these normal tissues interferes with the detection of tumors in the vicinity.

Lindholm et al. compared the uptake of FDG with the uptake of the amino acid L-[ $^{11}\text{CH}_3$ ] methionine (MET) in head and neck cancer (15). Their results showed that there were no significant differences with tumor imaging between MET and FDG, and that both tracers were very useful in the diagnosis of head and neck cancer. Braams et al. studied the uptake of TYR in cervical lymph nodes in head and neck cancer and found a better specificity and accuracy with TYR than with FDG, as previously reported (14).

In order to enable an earliest possible treatment of squamous cell carcinoma (SCC) it is important to know at which point of development PET can detect the disease. It is

known that oral epithelial dysplasia can be a preliminary state of SCC. We addressed this question with FDG and TYR in an oral dysplasia animal model. Oral epithelial dysplasia and SCC can be induced on the mucosa of the hard palate of the rat by repeated application of the carcinogen 4-nitroquinoline 1-oxide (4NQO). This autologous tumor model has advantages over transplanted models because it closely mimics human dysplasia and SCC (16,17). Furthermore, the grade of dysplasia can be numerically expressed by use of the epithelial atypia index (EAI) as developed by Smith and Pindborg (18).

The aim of this study was to compare the potential value of PET-FDG and PET-TYR in the detection of oral dysplasia and cancer in the 4NQO rat palatal model.

### Materials and Methods

#### Animal model

Dysplasias and SCC's were induced by the application of the carcinogen 4NQO on the mucosa of the hard palate of male Wistar Albino rats. The palates of 8 weeks old rats were painted three times a week with 4NQO (0.5% w/v) solved in propylene glycol during a brief anesthesia with (a mixture) O<sub>2</sub>/Halothane/ethrane. After application the rats were deprived of water for two hours to minimize the dilution effect. The rats were housed under standard conditions and had standard rat pellets and water *ad lib*.

When 4NQO is applied 3 times a week, highly differentiated SCC will develop within approximately 26 weeks. During the application period the tumors will be preceded by dysplasia of the oral epithelium. In general the whole palatal mucosa is dysplastic. Tumors arise locally and when the application is continued multifocal tumors are seen. The grading of the dysplasia is characterized by the EAI and correlated well with the extent of the application period (19). This experimental dysplasia is comparable to the human dysplasia and can be graded according to the EAI (18). For this study 54 rats were divided in 9 groups of 6 rats. The application with 4NQO for these different groups was respectively 2, 4, 6, 8, 12, 16, 20, 26 and 30 weeks.

#### PET imaging

The camera used was a Siemens ECAT 951/31 whole body machine (Siemens CTI, Knoxville, USA). The device acquires 31 planes across an axial length of 10.8 cm (slice thickness 0.35 cm). The measured resolution of the system is 5 mm at full width at half maximum (FWHM) transaxially in the center of the field of view.

No-carrier-added FDG was synthesized with a radiochemical purity greater than 98% according to Hamacher et al (20). TYR was produced by a remote controlled synthesis of a non-carrier added method via a microwave induced Bücherer-Strecker



synthesis (radiochemical purity 99%).

A transmission scan of 15 minutes was performed. After the injection of FDG or TYR a dynamic emission scan of 40 minutes was made.

Calculation of the PET-data was performed after individually reorientation and addition of the images. Briefly, the last 3 sagittal frames were added. These added sagittal PET-images were individually reoriented to coronal and frontal planes in order to obtain a better view of the palate. The frontal planes containing the palate of the rat were added on an individual basis. A standardized elliptical region of interest (ROI) was drawn on the hot spot representing the area of highest accumulation of the palate. Tracer accumulation was measured using the standardized uptake values (SUV).

$$\text{SUV} = \frac{\text{Radioactivity conc in ROI [mCi cm}^{-3}\text{]}}{\text{Injected dose [mCi]/Body weight [g]}}$$

### Experimental procedure

Five rats died during the anesthesia procedure. The PET experiments were repeated with five other rats with an equivalent 4NQO treatment period at a later moment.

For every stage of dysplasia and SCC 3 rats were investigated with FDG and 3 with TYR. Previous to the PET experiment the fasting rats were anaesthetized with an intraperitoneal injection of sodiumpentobarbital (Euthesate<sup>®</sup>). Three rats at the same time were positioned and fixed with tape in the camera on a what-not. Immediately after the transmission scan, FDG (range 0.2 to 0.5 mCi) or TYR (range 0.3 to 0.5 mCi) was injected into a lateral tail vein. The dose, and therefore the injected volume, was determined by the efficacy of the production yield of the tracer. Data-acquisition was started directly after administration of the tracer.

After the PET-data acquisition the rats were sacrificed by an intracardial injection of sodiumpentobarbital. Subsequently the hard palate and a part of the soft palate were dissected and photographed. The dissected specimens were fixated in 4% w/v formalin and decalcified in a solution containing 25% w/v formic acid and 0.34 M trisodium-citrate-dihydrate for approximately 4 weeks. The degree of decalcification was checked by X-ray analysis. After demineralization, the specimens were routinely processed and paraffin embedded. Histological sections of 7  $\mu\text{m}$  were cut in a sagittal plane at five different areas of the palate, namely in the front of the first molar, through the first molar, through the second molar, through the third molar and behind the third molar. The sections were stained with heamatoxylin and eosin and examined by light microscop-

py. For each rat an independent observer (PGJN), unaware of the PET results, assessed the EAI.

**Assessment of the epithelial thickness**

During the analysis it became apparent that the epithelial thickness possibly influenced the tracer accumulation (21). As a result of the 4NQO treatment the thickness of the epithelial and keratin layer of the mucosa was increased. For that reason the thickness of both layers was assessed on the same histological slides used for EAI analysis by a morphometric system (Quantimed, Cambridge systems, Cambridge, UK). For each rat the average of 3 measurements were used.

**Results**

**Macroscopic findings**

During the whole experiment the palats of the rats showed increasing changes of the mucosa. Up to eight weeks of 4NQO application no gross macroscopic changes were observed at the palatal mucosa. From that time a change of color of the palate to a more whitish aspect was detected. This whitening is probably the result of an increased keratinization and mild thickening of the mucosa. The topography of the palatal rugae was hardly disturbed. From that time on, the whitish thickening of the palatal mucosa increased and a slight loss of definition appeared as short ridges and papillary growth all over the palatal mucosa.

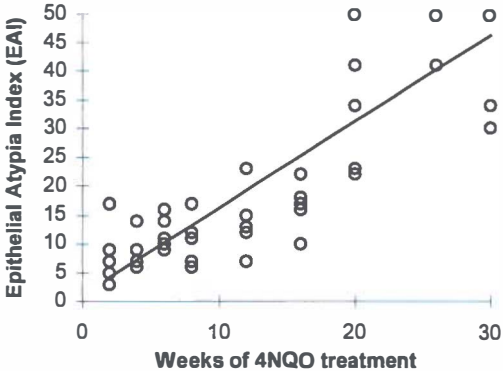


Figure 1. Results of histological analysis of rat palatal mucosa treated with 4NQO using the Epithelial Atypia index (EAI). The correlation between the application period and the increase of dysplasia was 0.84 (n=54).

The rugal topography however was still discernable. As a result of the continuous application of 4NQO the loss of normal structure gradually progressed. At week 26, exophytically growing epithelial lesions were observed. These lesions clinically presented as squamous-cell carcinomas and were most pronounced in the gingival areas of the palate. These macroscopical results are conform to the results of Nauta (21).

#### Microscopical findings

The histological changes of the palatal mucosa were graded with the use of the EAI. The EAI of 4NQO-untreated rats was zero, indicating a total absence of epithelial dysplasia. In figure 1 the EAI of the palatal mucosa is plotted against the weeks of 4NQO treatment. The EAI does not allow grading of SCC and therefore the number 50 was attributed to those palates of which the mucosa contained SCC. This is allowed because the Spearman test was used which analyzes rank order. A good correlation relationship was present between the 4NQO application period and the EAI (Spearman analysis of rank order, correlation coefficient = 0.84,  $p = 0.0001$ ). These results are in agreement with previous experiments with this tumor model (21).

During histological analysis it became apparent that the thickness of the epithelial layer was relevant to the amount of uptake. For that reason we measured the epithelial thickness of the 4NQO treated palatal mucosa. The correlation between the 4NQO treatment period and the increase of the epithelial thickness was 0.75 (Spearman analysis of rank order,  $p < 0.0001$ ). In absolute measures the thickness of the epithelial layer increased from 81  $\mu\text{m}$  (normal untreated mucosa) to as much as 770  $\mu\text{m}$  (mucosa treated for 30 weeks with 4NQO).

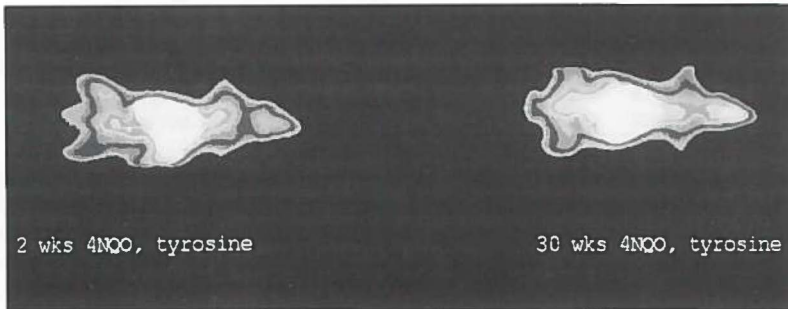


**Figure 2.** A PET-TYR image of two rats. A clear difference is visualized between the palate of the left rat (2 weeks 4NQO treated) and the right rat (30 weeks 4NQO treated) .

## PET analyses

On the PET images the palate was easy to locate due to the anatomical shape. There was no interference with the tracer uptake in the brain. The region of interest was any visually positive hot spot in the area of the palate. From the images it appeared as if a clear difference between slight dysplastic mucosa and severe dysplasia or SCC could be observed (fig 2). However, a difference in uptake of FDG or TYR could not be confirmed by statistical analysis of the SUVs among the 9 4NQO-treatment groups (Student Newman Keuls test).

With the use of FDG no relationship was found between the SUV of FDG and the EAI of the palatal mucosa (fig 3). Remarkable was the capricious pattern of SUVs of the rats injected with FDG. In this group the lowest mean SUV was found in the rats treated for 20 weeks with 4NQO while the highest mean SUV was found in rats treated for 12 weeks.

There was no correlation found between the SUV-FDG and the epithelial thickness (fig 4).

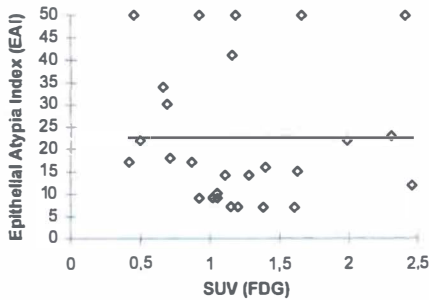


**Figure 3.** A plot of the standardized uptake values of FDG vs the degree of dysplasia (EAI). No correlation could be calculated. (n=27). Line indicates trend of data.

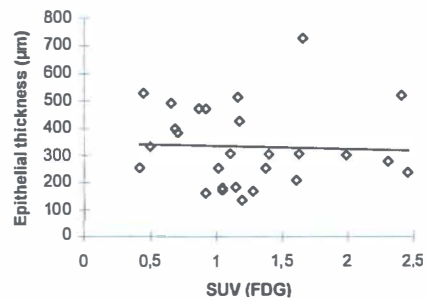


**Figure 4.** A plot of the standardized uptake values of FDG vs the epithelial thickness ( $\mu\text{m}$ ). No correlation could be calculated. (n=27). Line indicates trend of data.

With the tracer TYR, statistical analysis showed that a correlation of 0.5 (Spearman analysis of rank order,  $p < 0.0001$ ) existed between the SUV-TYR and the EAI (fig 5).

Furthermore, a correlation of 0.74 was found between the SUV-TYR and the increase of the epithelial thickness (Spearman analysis of rank order,  $p < 0.0001$ ) (fig 6).

## Discussion

In this paper we studied the efficacy of PET-FDG and PET-TYR for the detection of dysplasia and oral SCC in an animal model. The induction of dysplasia and SCC in the palatal mucosa by 4NQO is accompanied by inflammatory reactions. In the first weeks the inflamed tissues react with an increase of cellular response (22). There often is an increase of production of nasal fluids during the period of 4NQO induction. The presence of these tissue reactions may have influenced the FDG uptake. It has been well documented that FDG also accumulates in inflamed tissues (2-4). The histological slides showed in some rats with a high FDG-SUV clear signs of inflammation. This inflammation was mainly located at the basal membrane of the epithelium (fig 7). These reactions also declare the capricious FDG uptake pattern. Because no correlation between the SUV-FDG and the EAI was observed, it is concluded that FDG is not applicable as tracer for the detection of dysplasia in the 4NQO rat palatal tumor model.

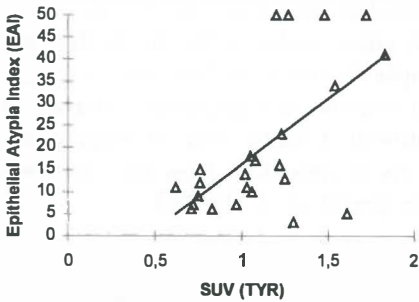


**Figure 5.** A plot of the standardized uptake values of TYR vs the degree of dysplasia (EAI). A correlation of 0.5 was calculated. (n=27).  
Line indicates trend of data.

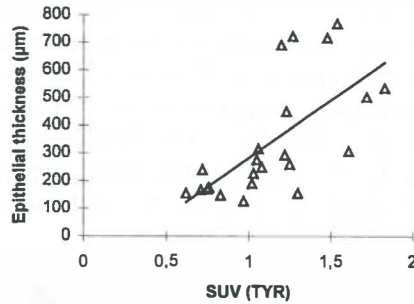


**Figure 6.** A plot of the standardized uptake values of TYR vs the epithelial thickness ( $\mu\text{m}$ ). A correlation of 0.74 was calculated. (n=27).  
Line indicates trend of data.

In contrast to SUV-FDG, the SUV-TYR showed a correlation with the EAI. The uptake of TYR was apparently less influenced by the presence of inflammatory tissue than the uptake of FDG. Because of the involvement of TYR in the protein synthesis this was expected. Several investigations showed the selectivity of amino acids in cancer cells (13). However, two studies also showed the uptake of the amino acid MET in inflamed tissue (23,24).

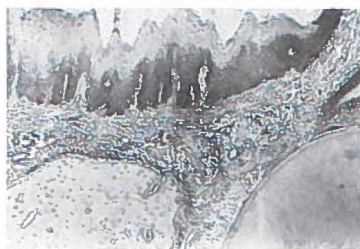


**Figure 7.** Photomicrograph of histological section of a rat palate treated for 12 weeks with 4NQO ( $\times 100$ ). This rat showed a high uptake of FDG at the palate, despite the slight dysplastic changes. The histological slide shows areas of clusters of inflammatory cells (arrows) and a diffuse spread of inflammatory cells in the stroma, probably responsible for the high FDG uptake.

A higher correlation was found between the thickness of the epithelial layer and the SUV-TYR than between the EAI and the SUV-TYR (0.74 versus 0.5). This remarkable difference was not anticipated. The increase of epithelial thickness due to the 4NQO treatment was comparable to the increase reported in other studies (19). As is shown in fig. 5 the high uptake of TYR occurred also in hyperplastic tissue without severe dysplastic characteristics. Apparently the increased protein demand in hyperplastic tissue was visualized by TYR-PET. The histological slides showed a large area of hyperplastic tissue (fig.8). It appeared that tissue hyperplasia is more important than the malignant features of dysplastic mucosa. No such correlation was found for FDG-PET.

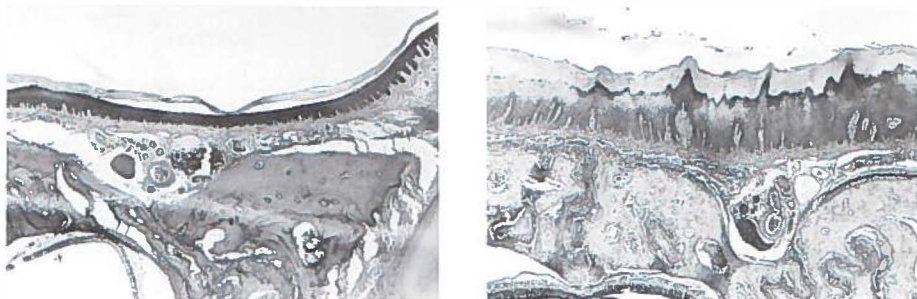


**Figure 8 A&B.** Photomicrographs of histological sections of (A) a normal rat palate and (B) a rat palate treated for 2 weeks with 4NQO (both  $100\times$ ). The 4NQO treated rat showed an remarkably high uptake of TYR at the palate. The histological slide showed an immoderate reactive hyperplasia, without inflammation, of the epithelium due to the 4NQO treatment. Normally, the dimensions of the epithelial layer in a rat treated for 2 weeks with 4NQO are similar to the dimensions of normal epithelium.

Despite of the small dimensions of the rat, the palate was easy to locate on the PET-images. It can be argued that due to the resolution of the PET camera, small malignant tumors can not be visualized. In this study we added three consecutive planes to obtain a clear picture of the palate of the rat. On average, the true dimensions of the palate is approximately  $0.5 \times 1 \text{ cm}^2$ . The thickness of the epithelial layer varied from approximately  $80 \text{ }\mu\text{m}$  to  $770 \text{ }\mu\text{m}$ , depending on the 4NQO treatment period. This implies that the true volume of the investigated tissue was approximately  $0.04 \text{ cm}^3$  to  $0.39 \text{ cm}^3$ . The selectivity of TYR for hyperplastic tissue was relatively good considering these small volumes. The results of FDG showed that this tracer cannot be applied in such small volumes. Due to the 4NQO induced inflammation, the quantification of the FDG uptake was not reliable.

With PET it is possible to detect severe dysplasia or early invasive carcinoma. It would be desirable that the uptake values beyond a certain threshold value would imply severe dysplasia or early carcinoma.

In this study a cut-off-point can be determined only for TYR. A SUV of 1.4 or higher would imply the presence of severe dysplasia or early invasive cancer (fig 5). Using this cut-off-point a sensitivity of 80% and a specificity of 89% can be calculated. However, whether the results of this rat experiments can be extrapolated to the human situation remains unclear. All dysplasia induced by 4NQO will eventually turn into invasive carcinoma whereas in humans dysplasia (leucoplakia) does not always becomes invasive carcinoma (21).

### **Conclusion**

Based on these experiments it can be concluded that only the uptake of TYR and not of FDG correlated well with the grade of oral dysplasia and SCC. However, TYR uptake proved to correlate better with tissue hyperplasia than with the degree of malignancy. Also in the 4NQO model PET-FDG suffered from high false positive results due to the uptake in inflamed tissues. These results are in accordance with our clinical experience with PET-FDG and PET-TYR.

## References

- 1 Conti PS, Lilien DL, Hawley K, et al. PET and [<sup>18</sup>F]-FDG in oncology: A clinical update. *Nucl Med Biol* 1996;6:717-735.
- 2 Sasaki M, Ichiya Y, Kuwabara Y. Ringlike uptake of [<sup>18</sup>F]FDG in brain abscess: a PET study. *J Comput Assist Tomogr* 1990;14:486-487.
- 3 Kubota R, Yamada S, Kubota K, Ishiwata K, Tamahashi N, Ido T. Intratumoral distribution of fluorine-18-fluorodeoxyglucose in vivo: high accumulation in macrophages and granulation tissues studied by microautoradiography. *J Nucl Med* 1992;33:1972-1980.
- 4 Wahl RL, Fisher SJ. A comparison of FDG, L-methionine and thymidine accumulation into experimental infections and reactive lymph nodes. *J Nucl Med* 1993;34:104P.
- 5 Ishiwata K, Takahashi T, Iwata R, et al. Tumor diagnosis by PET: potential of seven tracers examined in five experimental tumors including an artificial metastasis model. *Nucl Med Biol* 1992;19:611-618.
- 6 Hawkins RA, Phelps ME, Huang SC. Effects of temporal sampling, glucose metabolic rates and disruptions of the blood-brain barrier on the FDG model with and without a vascular compartment: studies in human brain tumors with PET. *J Cereb Blood Flow Metab* 1986;6:170-183
- 7 Di Chiro G. Positron emission tomography using [<sup>18</sup>F]fluorodeoxyglucose in brain tumors, a powerful diagnostic and prognostic tool. *Invest Radiol* 1987;22:360-371.
- 8 Ericson K, Lilja A, Bergstrom M, et al. Positron emission tomography with ([<sup>11</sup>C]methyl)-L-methionine, [<sup>11</sup>C]D-glucose, and [<sup>68</sup>Ga]EDTA in supratentorial tumors. *J comput Assist Tomogr* 1985;9:683-689.
- 9 Jabour BA, Choi Y, Hoh CK, et al. Extracranial head and neck: PET imaging with 2-[F-18]fluoro-2-deoxy-D-glucose and MR imaging correlation. *Radiology* 1993; 186:27-35.
- 10 Braams JW, Pruijm J, Freling NJM, et al. Detection of lymph node metastases of squamous cell cancer of the head and neck with FDG-PET and MRI. *J Nucl Med* 1995;36:211-216.
- 11 Vaalburg W, Coenen HH, Crouzel C, et al. Amino acids for the measurement of protein synthesis in vivo by PET. *Nucl Med Biol* 1992;19:227-237.
- 12 Phelps ME, Barrio JR, Huang SC, Keen RE, Chugani H, Mazziotta JC. Criteria for the tracer kinetic measurement of cerebral protein synthesis in humans with positron emission tomography. *Ann Neurol* 1984;15(suppl):S192-S202.
- 13 Willemsen ATM, van Waarde A, Paans AMJ et al. In vivo protein synthesis rate determination in primary or recurrent brain tumors using L-[<sup>11</sup>C]-Tyrosine and PET. *J Nucl Med* 1995;36:411-419.
- 14 Braams JW, Pruijm J, Nikkels PGJ, et al. Nodal spread of Squamous cel carcinoma of the oral cavity detected with PET-Tyrosine, MRI and CT. *J Nucl Med* 1996;37:897-901.
- 15 Lindholm P, Leskinen-Kallio S, Minn H, et al. Comparison of fluorine-18-fluorodeoxyglucose and carbon-11-methionine in head and neck cancer. *J Nucl Med* 1993;34:1711-1716.
- 16 Nauta JM, Roodenburg JLN, Nikkels PGJ, Witjes MJH, Vermey A. Comparison of epithelial dysplasia. The 4NQO rat palatal model versus human oral mucosa. *Int J Oral Maxillofac Surg* 1995;24:53-58.
- 17 Prime SS, Malamos D, Rosser TJ, Scully CM. Oral epithelial atypia and acantholytic dyskeratosis in rats painted with 4-nitroquinoline N-oxide. *J Oral Pathol* 1986;15:280-283.



- 18 Smith CJ, Pindborg JJ. Histological grading of oral epithelial atypia by the use of photographic standards. C. Hamburger, Copenhagen 1969.
- 19 Nauta JM, Roodenburg JLN, Nikkels PGJ, Witjes MJH, Vermey A. Epithelial dysplasia and squamous cell carcinoma of the wistar rat palatal mucosa. The 4NQO model. *Head and Neck* 1996;18:441-449.
- 20 Hamacher K, Coenen HH, Stöcklin G. Efficient stereospecific synthesis of no-carrier-added 2-<sup>[18F]</sup>-fluoro-2-deoxy-D-glucose using aminopolyether supported nucleophilic substitution. *J Nucl Med* 1986;27:235-238.
- 21 Nauta JM. Photodynamic therapy and photodetection of dysplastic lesions and squamous cell carcinomas of the oral mucosa. Thesis, University of Groningen, Groningen: van Denderen 1996.
- 22 Fisker AV. Chemically induced experimental oral carcinogenesis. Establishment of an experimental model based on application of the carcinogen 4-nitroquinoline n-oxide on the palatal mucosa of rats. PhD Thesis Royal Dental College, Aarhus. Denmark 1978.
- 23 Leskinen-Kallio S, Nägren K, Lehtikoinen P, Ruotsalainen U, Joensuu H. Uptake of <sup>11</sup>C-methionine in breast cancer studied by PET. An association with the size of S-phase fraction. *Br J Cancer* 1991;64:1121-1124.
- 24 Kubota K, Matsukawa T, Fujiwara T, et al. Differential diagnosis of lung tumor with positron emission tomography: a prospective study. *J Nucl Med* 1990;31:1927-1933.



- CHAPTER 7 -

**DETECTION OF UNKNOWN PRIMARY HEAD AND NECK TUMORS  
WITH THE USE OF POSITRON EMISSION TOMOGRAPHY**

Jan Willem Braams, Jan Pruim, Annemiek C. Kole, Peter G.J. Nikkels,  
Willem Vaalburg, Albert Vermey, Jan L.N. Roodenburg.

Departments of:     Oral and Maxillofacial Surgery  
                          PET center  
                          Surgical Oncology  
                          Pathology

Groningen University Hospital, Groningen, The Netherlands.

The purpose of this study was to investigate the potential of using positron emission tomography (PET) with  $^{18}\text{F}$ -fluoro-2-deoxy-D-glucose (FDG) for the detection of unknown primary tumors of cervical metastases. **Methods:** Thirteen patients with various histologic types of cervical metastases of unknown primary origin were studied. Patients received 185 to 370 MBq FDG intravenously and were scanned from 30 minutes after injection onwards. Whole body scans were made with a Siemens ECAT 951/31 PET-camera. **Results:** PET identified the primary tumor in four patients: a plasmocytoma, a squamous cell carcinoma of the oropharynx, a squamous cell carcinoma of the larynx and a bronchial carcinoma. All known metastatic tumor sites were visualized. PET did not identify a primary tumor in one patient in whom a squamous cell carcinoma at the base of the tongue was found in a later phase. In the remaining eight patients a primary lesion was never found. The follow-up ranged from 18 to 30 months. **Conclusions:** A previously unknown primary tumor can be identified with FDG-PET in approximately 30 percent of patients with cervical metastases. PET can reveal useful information that results in more appropriate treatment. PET can be of value in guiding endoscopic biopsies for histological diagnosis.

## Introduction

Patients with an unknown primary cancer represent 5% to 10% of all cancer patients (1). Within this heterogeneous group of patients there are various clinical presentations, while the primary tumors may have a different histologic pattern.

The location of the involved lymph nodes may give an indication about the location of the primary tumor. When the lymph nodes of the upper and middle cervical level are involved, a primary tumor in the head and neck region is more likely. In case the lower cervical lymph nodes are involved, the primary tumor is often located below the clavicles.

In 2 to 4 percent of patients presenting with metastatic squamous cell carcinoma (SCC) in cervical lymph nodes, a primary site can not be identified during the diagnostic phase of the clinical course. In these patients most primary sites become manifest in the head and neck region (1).

In case of SCC metastases in the upper and middle cervical nodes without a known primary tumor, the most common treatment consists of radical or modified radical neck dissection and postoperative radiotherapy of both sides of the neck and all possible primary tumor sites, including the nasopharynx. Unfortunately, the morbidity of the treatment is rather severe and includes xerostomia, mucosal atrophy, and the inherent risk of osteoradionecrosis of the jaws. The detection of the primary location is, therefore, of great significance because it probably will limit the extent of the treatment and thus, reduce the unwanted side effects.

In the diagnostic workup to detect the primary tumor, endoscopy is the keystone. Magnetic resonance imaging (MRI) and computed tomography (CT) are also commonly used to try to visualize the unknown primary tumor and their use have already been evaluated (2-5).

An alternative way of cancer imaging is to study the physiochemical properties of tumor cells. It has been shown that malignant cells have an increased glucose consumption due to an increased glycolysis. The increased glycolysis can be monitored with positron emission tomography (PET) using  $^{18}\text{F}$ -fluoro-2-deoxy-D-glucose (FDG). FDG-PET has been applied for detection and staging of different types of cancer including head and neck SCC (6-10). FDG-PET showed a relatively high sensitivity and a moderate specificity for the detection of metastatic lymph nodes of SCC in the neck as compared to MRI. The smallest metastatic lymph node detected with FDG-PET was 4 mm (6). Based on these findings it was hypothesized, that unknown primary tumors in patients with cervical metastases may be detected with FDG-PET. The aim of this study was to investigate the potential of positron emission tomography with respect to this hypothesis.

## Materials and Methods

### Patients

Thirteen patients, 3 women and 10 men, with a mean age of 58 yrs (42 - 77 yrs) were studied. All patients were submitted to the Head and Neck Cooperative Oncology Group of the Groningen University Hospital for evaluation of metastatic lymph nodes of the neck region with an unknown primary tumor.

All patients underwent a physical examination and were evaluated with MRI and/or CT of the head and neck area. When no primary tumor was found a FDG-PET investigation was performed. Written informed consent was obtained from all patients. The study was approved by the Medical Ethics Committee of the Groningen University Hospital.

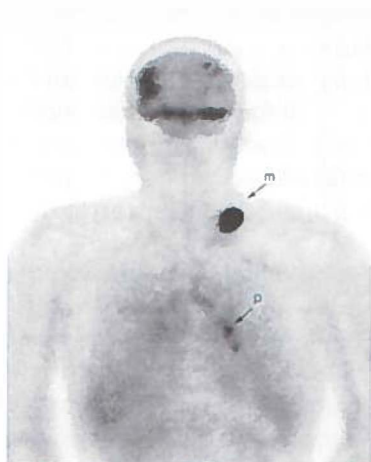


**Figure 1.** An example of detection of an unknown primary tumor: metastasis (m), primary tumor (p) (17).

### Experimental setup

FDG was synthesized using the method described by Hamacher et al. (11) with a radiochemical purity of more than 98%. The PET-camera used was a Siemens ECAT 951/31 whole body machine. This device acquires 31 planes over an axial length of 10.8 cm. The measured resolution of the system is 6 mm full width at half maximum (FWHM)

transaxially in the center of the field of view. The patients were fasted overnight before the PET study. Whole body scans were made 30 minutes after administration of 185-370 MBq (5-10 mCi) FDG into a peripheral vein of one of the upper extremities. Depending on the length of the patient 17 - 22 bed positions of 3 minutes each were scanned to cover the whole body. Images were visually assessed using standard ECAT software. Depending on the location any positive hot spot on the whole body scan was considered to be the primary tumor or another possible metastases.

After the PET, an endoscopy of the oropharynx, hypopharynx, nasopharynx, larynx, and upper part of the esophagus was performed under general anaesthesia. Suspected areas were biopsied. The endoscopist was blinded for the PET results. In case PET indicated a primary tumor in the head and neck region and no primary tumor was found during endoscopy, a second endoscopy was performed to obtain histology from the area concerned.

## Results

For all patients, the diagnosis 'metastasis of unknown primary tumor' was made after fine needle aspiration cytology and/or histopathology after neck dissection (Table I). Ten patients suffered from metastasis of a SCC of unknown origin. The histology of the other 3 patients was adenocarcinoma, plasmocytoma and a papillary thyroid carcinoma.

In 4 of 10 patients with an unknown primary SCC, the primary tumors were found either after endoscopy (tongue, size 4 mm) or PET analysis (larynx, size 5 mm, oropharynx, size 6 mm, and lung, size unknown). Of the three PET positive cases, endoscopy confirmed the presence of a SCC in the larynx and the oropharynx, respectively. In the third patient endoscopy could not confirm the diagnosis of the primary tumor in the lung as indicated by PET. One SCC found by endoscopy at the base of the tongue was not observed by PET analysis. These four patients were treated by surgery and/or radiotherapy. The follow up period varies from 12 to 16 months. Of these four patients, three have died due to their cancer.

In the other 6 patients from the group of 10 with SCC, no primary SCC was found with either FDG-PET or endoscopy. These patients received standard treatment and follow up. During the follow up period of 18 to 27 months no primary tumor or regional recurrence occurred. One patient died during the follow up period from cardiac arrest, 27 months after first presentation of the neck mass.

In the Non-SCC group a plasmocytoma of the tongue (size 3 mm) was found by PET analysis. This patient was treated by excision and the diagnosis was histopathologically proven. The patient is still alive and considered cured at the time of submission of the manuscript. In the two other patients no primary tumor was identified and patients received standard treatment and follow up. The follow up period of these three patients

varied from 28 to 31 months, without any sign of a primary tumor or recurrence.

Of the nine patients with cervical metastases at a high level (i.e. the upper 2/3 of the neck), 3 of 4 primary tumors were retrieved. Of the four patients with cervical lymph nodes at a low level 1 unknown primary was found with FDG-PET.

**Table 1.** Localisation of metastases and the detected primary tumor, H = high level, L= low level.

nr	sex	metastases			primary tumor				
		histology cytology	level	localisation	tumor size (mm)	endo- scopy	PET	endoscopy after PET	broncho- scopy
1	m	scc	H	tongue	4	+	-		
2	m	scc	H	larynx	5	-	+	+	
3	m	scc	H	oropharynx	6	-	+	+	
4	m	scc	L	lung	-	-	+		-
5	f	scc	L	-	-	-	-		
6	m	scc	H	-	-	-	-		-
7	m	scc	H	-	-	-	-		
8	m	scc	H	-	-	-	-		
9	m	scc	H	-	-	-	-		
10	m	scc	H	-	-	-	-		
11	m	adeno	L	-	-	-	-		
12	f	plasma- cytoma	H	tongue	3	-	+	+	
13	f	papillary	L	-	-	-	-		

## Discussion

In this study we explored the potential of FDG-PET for diagnosing primary unknown tumor sites. Unknown primary tumors are a heterogeneous group of tumors with widely varying natural histories. Patients with unknown primary tumors have a poor median survival of 3 to 4 months, with less than 25% of patients alive 1 year after diagnosis and less than 10% survival at 5 years (12-15). The background of our study was the assumption that the prognosis of a patient with a metastasis of unknown origin may increase when the primary tumor is found and thus, more specific treatment can be performed.

After their introduction in general clinical practice, CT and MRI generally have greatly improved diagnosing the presence of metastatic (lymph node) disease. A major drawback, however, is that both techniques rely on structural alterations. Within the



context of metastatic lymph node disease, size of a lymph node is a major criterion as shown by van den Brekel et al.(2). The larger the node the higher the chance of metastatic disease. In order to improve specificity, size criteria are chosen at the cost of a lower sensitivity. However, it is well known that larger nodes may not contain metastatic cells (false positives), whereas smaller nodes may still contain metastases (false negatives). For instance, nearly 40% of enlarged mediastinal lymph nodes (2-4 cm in diameter) in newly diagnosed lung cancer patients do not harbour tumour cells, as shown by McLoud et al.(16). Consequently, a fundamentally different approach is needed to detect metastatic lymph node disease.

PET is a technique based on the visualization (and quantification) of metabolism rather than anatomy. Since tumor cells differ in their metabolism, a.o. glucose utilization, from normal cells, the technique has been applied in oncology with good results (6-10). The unfavourable resolution of PET (approx. 5 mm in current cameras) as compared to MRI (1 mm) can be overcome by a favourable tumor-to-background ratio and the lack of rigid criteria to improve specificity. In the head and neck tumor locations of 4 mm have been detected, which compares favourable with MRI in which a node size of 8-10 mm is considered to be the borderline.

Minn, et al. described the uptake of FDG in malignant head and neck tumors and metastases (9). Wahl, et al. reported that FDG has potential as a radiopharmaceutical agent for detection of metastatic tumors in regional lymph nodes using PET scanning (10). Braams, et al. described that with the use of FDG-PET metastatic lymph nodes can be detected with a high sensitivity and specificity (6). In all of these studies there was clear evidence of a primary tumor which contrasts with the current study in which the clinical applicability of FDG-PET for the detection of a unknown primary tumor in patients with cervical metastases was investigated

In the total group of 8 patients with cervical metastases of SCC at a high level 3 unknown primary tumors were found; 2 with PET and one by endoscopy. In the follow up period of the 5 other patients no primary tumour was ever found. A primary tumor of the base of the tongue (size 4 mm) was missed by PET. This primary tumor was later diagnosed by a second endoscopy. It can be argued that because of the relatively small size of the tumor, the tumor could not be detected with PET. It is also likely, that a small tumor may manifest itself by a superficial inflammatory reaction, so it is easier to detect with endoscopic examination than with PET. This is one of the advantages of the endoscopic examination.

In 4 patients the cervical metastases were situated at a low level. In one patient a primary SCC of the lung was visualized with PET. Other diagnostic modalities failed to visualize this primary lung tumor.

In the group of three non squamous cell carcinomas one primary tumor was found; a plasmocytoma of the tongue. The plasmocytoma was not visualized by any other

imaging modality or endoscopy. Based on the PET-findings excision followed and the patient is considered to be cured. In this patient the additional value of PET became obvious. The locations of the primary tumors varied from tongue, larynx, oropharynx to lung. It is therefore, advisable to examine the whole body with FDG-PET in the search for a primary tumor, especially when the metastases are located in the lower level of the neck.

Six patients with a metastases of a SCC in whom PET failed to identify the primary tumor, remained free from primary manifestation after a follow up period of 18 to 30 months. These patients did well after the standard treatment, although the follow up period is still rather short.

It is concluded that FDG-PET may be of additional value in the detection of the unknown primary tumor, but the technique has its limitations because relatively small tumors (< 4 mm) cannot be detected.

## References

- 1 Greco FA, Hainsworth JD. Cancer of unknown primary site. In DeVita VT, Hellman S, Rosenberg SA, eds.: *Cancer: Principles & Practice of Oncology*, Fourth edition. Philadelphia: J.B. Lippencott Co. 1993;2072-2092.
- 2 Brekel MWM van den, Stel HV, Castelijns JA, et al. Cervical lymph node metastasis: assessment of radiologic criteria. *Radiology* 1990;177:379-384.
- 3 Karsell PR, Sheedy PF, O'Connell MJ. Computerized tomography in search of cancer of unknown origin. *JAMA* 1982;248:340-343.
- 4 McMillan JH, Levine E, Stephens RH. Computed tomography in the evaluation of metastatic adenocarcinoma from an unknown primary site. *Radiology* 1982;143:143-146.
- 5 Steinkamp HJ, Knöbber D, Zwicker C, et al. Halslymphknotenmetastasen bei unbekanntem primärtumor: Gibt es eine bildgebende Differentialdiagnostik? *Laryngo Rhino Otol* 1993;72:78-85.
- 6 Braams JW, Pruim J, Freling NJM, et al. Detection of lymph node metastases of squamous-cell cancer of the head and neck with FDG-PET and MRI. *J Nucl Med* 1995;36:211-216.
- 7 Haberkorn U, Strauss LG, Reisser Ch, et al. Glucose uptake, perfusion and cell proliferation in head and neck tumors: relation of positron emission tomography to flow cytometry. *J Nucl Med* 1991;32:1548-1555.
- 8 Jabour BA, Choi Y, Hoh CK, et al. Extracranial head and neck; PET imaging with 2-[F-18]fluoro-2-Deoxy-D-glucose and MR imaging correlation. *Radiology* 1993;186:27-35.
- 9 Minn H, Joensuu H, Ahonen A, Klemi P. Fluorodeoxyglucose imaging: a method to assess the proliferative activity of human cancer in vivo. *Cancer* 1988;61:1776-1781.
- 10 Wahl RL, Kaminski MS, Ethier SP, Hutchins GD. The potential of 2-deoxy-2[18F]fluoro-D-glucose (FDG) for the detection of tumor involvement in lymph nodes. *J Nucl Med* 1990;31:1831-1835.
- 11 Hamacher K, Coenen HH, Stöcklin G. Efficient stereospecific synthesis of no-carrier-added 2-[18F]-fluoro-2-deoxy-D-glucose using aminopolyether supported nucleophilic substitution. *J Nucl Med* 1986;27:235-238.
- 12 Abbruzzese JL, Abbruzzese MC, Hess KR, et al. Unknown primary carcinoma: Natural history and prognostic factors in 657 consecutive patients. *J Clin Oncol* 1994;12:1272-1280.
- 13 Holmes FF, Fouts TL. Metastatic cancer of unknown primary site. *Cancer* 1970;26:816-820.
- 14 Richardson RG, Parker RG. Metastases from undetected primary cancers: Clinical experience at a radiation oncology center. *West J Med* 1975;113:337-339.
- 15 Smith PE, Kremenz ET, Chapman W. Metastatic cancer without a detectable primary site. *Am J Surg* 1967;113:633-637.
- 16 Mcloud TC, Bourgouin PM, Greenberg RW, et al. Bronchogenic carcinoma: Analysis of staging in the mediastinum with CT by correlative lymph node mapping and sampling. *Radiology* 1992;182:319-323.
- 17 Kole AC, Nieweg OE. Toepassingen van positron-emissietomografie in de oncologie. *Ned Tijdschr Geneesk* 1996;140:244-248.



- CHAPTER 8 -

SUMMARY  
AND  
GENERAL DISCUSSION

## 8.1 Introduction

PET has the ability to image physiological processes with the use of radioactive tracers like radiolabeled glucose derivatives and amino acids. In head and neck oncology, the extent of the tumor and the presence or absence of lymph node metastases determine the treatment and the prognosis of the patient. With the clinical application of PET using the tracers 2-deoxy-2-[<sup>18</sup>F]fluoro-D-glucose (FDG) and L-[1-<sup>11</sup>C]-tyrosine (TYR), it became possible to reflect the increased glycolysis and protein synthesis rate in primary tumors and metastases. In this thesis investigations are presented whether PET by use of these tracers can be of help in the detection of cervical lymph node metastases and unknown primary tumors.

## 8.2 The assessment of metastatic lymph nodes

The chapters 3, 4 and 5 are dedicated to the assessment of the presence of cervical lymph node metastases from primary squamous cell carcinoma's (SCC's) in the oral cavity. Detection of occult metastases is clinically important, since the extent of the treatment is determined by the presence or absence of such metastatic lymph nodes. Several investigators have sought for more accurate imaging techniques that will allow better assessment of cervical metastatic lymph nodes (1). It can be concluded that computed tomography (CT)(sensitivity 83%, specificity 70%), magnetic resonance imaging (MRI)(sensitivity 82%, specificity 81%) and ultrasound (US)(sensitivity 75%, specificity 75%) give better results as compared with palpation in detecting or excluding metastatic neck disease (1). Until now US-guided fine needle aspiration cytology (FNAC) in well trained hands (sensitivity 90%, specificity 100%) seems to be the most sensitive, specific and accurate technique to detect or exclude metastatic neck disease in patients with SCC's preoperatively (1). However, in a multicenter trial reported by Takes et al. (2) the sensitivity of detecting metastatic lymph nodes in the neck decreased to 77%. In a very recent study this group reported a sensitivity of 48% in detecting lymph node metastases in a clinically negative neck.(3)

The main problems with US-guided FNAC are that no standardized permanent document is obtained and that the accuracy of the technique fully depends on the experience of the examiner.

We have explored the possibilities of PET for the detection of metastatic lymph nodes. First, we studied the applicability of FDG in the detection of lymph node metastases from primary SCC's in the oral cavity. With histology used as a reference PET found 20 of the 22 metastatic lymph nodes, resulting in a sensitivity of 91%. The specificity for PET-FDG was 88%. A severe drawback of PET-FDG was the uptake in inflammatory nodes. Also other investigators mentioned the uptake of FDG in inflammatory nodes or abscesses (4-6).

With the introduction of the amino acid TYR, a tracer became available to visualize the protein synthesis rate of tumor tissue (7). The sensitivity of 83% and a specificity of 95% for TYR-PET, compared favourably with the results of CT and MRI. Compared to PET-FDG findings TYR-PET had a better specificity (88% vs 95%), accuracy (88% vs 95%) and positive predictive value (48% vs 63%). However, there were more false negative results with TYR-PET. Another drawback with TYR-PET is the uptake in bone marrow and salivary glands. Especially the salivary glands are closely related to lymph nodes and this gives problems in identifying neighbouring lymph nodes.

For clinical PET studies FDG and TYR are two reliable tracers suitable for the detection of lymph node metastases of SCC's, because of the high negative predictive values. We prefer PET-FDG in patients with a clinically negative neck. Patients with palpable nodes in the neck should be scanned with TYR-PET because of the high accuracy, specificity and positive predictive value.

PET-imaging as applied in chapter 3 and 4 is rather cumbersome to the patient. It is time consuming and requires for the patient a long time of lying still (1.5 hr). To reduce this scanning-time with 1 hr we investigated the use of a whole-body scanning without transmission scan (chapter 5). PET scanning in the whole-body mode with the tracer TYR appears to be for the patient a more convenient technique with comparable results as obtained with the classical PET-TYR scanning. However, the problem of TYR uptake in the salivary glands and in bone marrow remains. Especially, the uptake in the salivary glands impairs the analysis of PET images.

### 8.3 In vivo measurement of dysplasia

In chapter 6 we investigated the uptake of FDG and TYR in rats palates with chemically induced dysplasia and SCC. PET-FDG seems not to be able to discriminate between the different stages of chemically induced dysplasia in palates of Wistar Albino rats. By the induction of dysplasia with 4-nitroquinoline 1-oxide (4NQO), the palatal mucosa will at first react with inflammatory lesions (8). It has been well documented that FDG also accumulates in inflammatory tissues (4-6). Between the uptake of FDG and the Epithelial Atypia Index (EAI) no correlation was found. So, it can be concluded that FDG is not suitable as a tracer for the detection of dysplasia in the 4NQO palatal rat tumor model.

In contrast to the uptake values for FDG, the uptake values for TYR showed a correlation with the EAI. Apparently, the uptake of TYR is less influenced by inflammatory tissues. The higher selectivity of labeled amino acids for cancer cells is described by several authors (7,9-11). However, there are reports which describe the uptake of amino acids in inflammatory tissues (10,11).

In our study we found a higher correlation of standardized uptake values of TYR (SUV-TYR) with the epithelial thickness, than between SUV-TYR and the EAI. After histological investigation of the palatal mucosa it appeared that the tissue hyperplasia is more important than the malignant features of the dysplastic mucosa.

It can be argued that this animal model is not ideal. Because of the resolution of the camera a tumor smaller than 6 mm can not be visualized. However, the statistical difference in TYR uptake values between an animal treated 4 weeks with 4NQO and an animal treated 30 weeks is significant.

For the clinical use of PET it would be desirable that severe dysplasia or early invasive carcinoma can be imaged by the uptake of the tracer beyond a certain threshold value. Whether the results of this animal study can be extrapolated to the human situation is yet unclear. In this study using a cut-off point of SUV 1.4 a sensitivity of 80% and a specificity of 89% can be calculated.

Based on these experiments it can be stated that only TYR has a correlation with experimental oral dysplasia and SCC. The best correlation was seen between PET-TYR and hyperplasia.



#### 8.4 Unknown primary tumors

In chapter 7 we investigated the detection of unknown primary tumors in patients with cervical lymph node metastases. In 30% of the patients with cervical metastases of an unknown primary, PET-FDG detected the previously unknown primary tumor. PET-FDG can be of value in guiding endoscopic biopsies for histological diagnosis. An endoscopic biopsy should always be taken after the PET-investigation, because the resulting wound healing reaction at the place of biopsy can give false positive results on the PET images. Despite these favourable results, the detection of unknown primary tumors by PET is hampered by the resolution of the camera. Therefore relatively small tumors (smaller than approx. 6 mm) cannot be detected. However PET-FDG can be of additional value in the detection of the unknown primary tumor. The value of PET-TYR for this indication also should be investigated because this tracer showed better results in the animal model.

#### 8.5 General discussion

Positron emission tomography (PET) is a new approach in the diagnostic workup in cancer patients. In contrast to palpation and imaging with CT, MRI and US, biochemical processes are monitored in the patient. Primary tumors as well as metastatic disease can be detected with PET.

Using FDG as a tracer, the glucose consumption of tissues can be studied. The tracer TYR gives insight in the cell protein synthesis of tissues. However, like every diagnostic modality PET has its limitations and drawbacks. These are partly due to the equipment and partly to the tracers used.

The equipment needed for PET requires not only a camera but also a cyclotron to produce short-lived radioactive tracers. This makes PET an expensive diagnostic modality and asks for well planned logistic procedures. The power of PET in head and neck oncology is the possibility of detection of metastatic lymph nodes between 5 and 10 mm in size and its adjunctive role in patients with unknown primary tumors. Only USgFNAC is cheaper but its value depends on the skills of the investigator. In comparison with now generally accepted methods (MRI,CT), which were also expensive in the experimental phase it may be expected that PET will be cheaper in near future.

The resolution of the camera is a limiting factor. The studies presented in this thesis claim the detection of metastatic lymph nodes with a size minimum between 4 and 6 mm, although even smaller lesions can be found by chance. In one occasion a plasmocytoma of 3 mm was found. In general, for reliable detection of metastatic lymph nodes a lesion should have a diameter of at least 5 mm. This size criterium is smaller than the size criteria for CT and MRI. Fortunately, this method need no special skills of the investigator like for example USgFNAC.

The tracers used, FDG and TYR showed both a high sensitivity but the specificity was influenced by several factors. PET-FDG showed false positives due to inflammatory lymph nodes, while TYR-PET was hampered by the uptake of this tracer in salivary gland tissue.

In case PET is combined with a transmission scan, this investigation takes about 1.5 hours and is therefore very cumbersome to some patients. This also results in a less cost-effective use of the equipment. Reducing the camera time by using wholebody mode and omitting the transmissionscan shows interesting results and may be a way to overcome the problem of a long camera time.

Based on our experience the bottom line for PET-FDG and TYR-PET in head and neck oncology is the detection of tumors and/or metastases with a minimum size of 6 mm. A reliable detection of premalignant lesions was not possible. In the search for unknown primary tumors PET-FDG may contribute to the more successful detection of unknown primary tumors.

This study showed that PET can be helpful in head and neck oncology in the following situations:

1. to confirm a negative neck in case of squamous cell carcinoma of the upper aerodigestive tract with PET-FDG, because of the high sensitivity and negative predictive value of PET-FDG.
2. to image (doubtful) positive necknodes of squamous cell carcinoma of the upper aerodigestive tract with PET-TYRWB, because of the high specificity, accuracy and predictive values.
3. to search for unknown primary tumors of cervical metastases with PET-FDG in whole body mode.

**References**

1. Van den Brekel MWM. Assessment of lymph node metastases in the neck. Thesis Free University Amsterdam, Utrecht: Elinkwijk 1992.
2. Takes RP, Knegt P, Manni JJ, Meeuwis CA, Marres HAM, Spoelstra HAA, et al. Regional metastasis in head and neck squamous cell carcinoma: revised value of US with US-guided FNAB. *Radiology* 1996;198:819-823.
3. Takes RP, Righi P, Meeuwis CA, Manni JJ, Knegt P, Baatenburg de Jong RJ, et al. The value of ultrasound with ultrasound-guided fine needle aspiration biopsy compared to computed tomography in the detection of regional metastases in the clinically negative neck. *Br J Cancer* 1998;77:16.
4. Tahara T, Ichiya Y, Kuwabara Y, et al. High [<sup>18</sup>F]fluorodeoxyglucose uptake in abdominal abscesses: a PET study. *J Comput Assist Tomogr* 1989;13:829-831.
5. Sasaki M, Ichiya Y, Kuwabara Y, et al. Ringlike uptake of [<sup>18</sup>F]FDG in brain abscess: a PET study. *J Comput Assist Tomogr* 1990;14:486-487.
6. Kubota R, Yamada S, Kubota K, Ishiwata K, Tamahashi N, Ido T. Intratumoral distribution of fluorine-18-fluorodeoxyglucose in vivo: High accumulation in macrophages and granulation tissues studied by microautoradiography. *J Nucl Med* 1992;33:1972-1980.
7. Ishiwata K, Kubota K, Murakami M. et al. Re-evaluation of amino acid-pet studies: can the protein synthesis rates in the brain and tumor tissues be measured in vivo ? *J Nucl Med* 1993;34:1936-1943.
8. Nauta JM, Roodenburg JLN, Nikkels PGJ, Witjes MJH, Vermey A. Epithelial dysplasia and squamous cell carcinoma of the wistar rat palatal mucosa. The 4NQO model. *Head and Neck* 1996;18:441-449.
9. Ishiwata K, Takahashi T, Iwata R, et al. Tumor diagnosis by PET: potential of seven tracers examined in five experimental tumors including an artificial metastasis model. *Nucl Med Biol* 1992;19:611-618.
10. Lindholm P, Leskinen-Kallio S, Minn H, et al. Comparison of fluorine-18-fluorodeoxyglucose and carbon-11-methionine in head and neck cancer. *J Nucl Med* 1993;34:1711-1716.
11. Leskinen-Kallio S, Någren K, Lehtikainen P, Ruotsalainen U, Joensuu H. Uptake of <sup>11</sup>C-methionine in breast cancer studied by PET. An association with the size of S-phase fraction. *Br J Cancer* 1991;64:1121-1124.

## SAMENVATTING

In de oncologie bepalen onder meer de uitbreiding van de primaire tumor en de aan- of afwezigheid van lymfkliermetastasen de behandeling en de prognose van de patiënt. Met behulp van Positron Emissie Tomografie (PET) in vivo kunnen metabole processen afgebeeld worden door gebruik te maken van radioactieve glucose derivaten en aminozuren. De klinische toepassing van PET in combinatie met de tracers  $^{18}\text{F}$ -fluoro-2-deoxy-D-glucose (FDG) en L-[1- $^{14}\text{C}$ ]tyrosine (TYR), maakt het mogelijk om respectievelijk de verhoogde glycolyse en eiwitsynthese in primaire tumoren en lymfkliermetastasen zichtbaar te maken. Het hier gepresenteerde werk beschrijft of PET met gebruikmaking van de twee eerder genoemde tracers geschikt is voor de detectie van cervicale lymfkliermetastasen uitgaande van een planocellulair carcinoom van de bovenste adem- en voedingsweg en van onbekende primaire tumoren.

De hoofdstukken 3, 4, en 5 zijn gewijd aan de detectie van cervicale lymfkliermetastasen van primaire planocellulaire carcinomen van de bovenste adem- en voedingsweg. Vele onderzoekers hebben gezocht naar meer accurate afbeeldingstechnieken, om cervicale metastasen af te beelden. De huidige methodes zoals CT en MRI geven goede resultaten in vergelijking met palpatie. Echogeleide punctie lijkt momenteel de methode met de hoogste sensitiviteit, specificiteit en accuratesse. Bij echogeleide punctie wordt echter geen gestandaardiseerd document verkregen en het onderzoek is sterk afhankelijk van de vaardigheid van de onderzoeker.

In deze hoofdstukken worden de mogelijkheden van PET voor de detectie van cervicale lymfkliermetastasen beschreven. PET wordt vergeleken met MRI en CT waarbij de pathologie als gouden standaard wordt gebruikt. Het grote verschil van PET met de andere afbeeldingstechnieken is dat wordt gekeken naar het metabolisme van cellen in plaats van naar anatomische structuren zoals bij CT en MRI. Dit is dan ook tevens het belangrijke nadeel: plaatsbepaling met PET is soms moeilijk.

Het blijkt dat PET met behulp van de tracers FDG en TYR in staat is om lymfkliermetastasen af te beelden. De minimale grootte van deze lymfklieren ligt tussen de 4 en de 6 mm. Op basis van deze gegevens zou PET een waardevolle toevoeging kunnen zijn bij het onderzoek van patiënten met een metastase uitgaande van een planocellulair carcinoom van het slijmvlies van de bovenste adem - en voedingsweg.

Het eerste onderzoek was gericht op de bruikbaarheid van PET met de tracer FDG voor de detectie van cervicale lymfkliermetastasen uitgaande van het slijmvlies van de bovenste adem- en voedingsweg. Met de histologie als referentie detecteerde PET 20 van de 22 metastasen. Dit resulteerde in een sensitiviteit van 91% en een specificiteit van 88%. Het nadeel van de tracer FDG bleek dat reactieve lymfklieren en of gebieden met een hoog metabolisme ook duidelijk afgebeeld werden. Het afbeelden van de reactieve lymfklieren heeft tot gevolg dat er relatief veel vals positieve resultaten waren. Het andere nadeel van opname in gebieden met een hoog metabolisme heeft tot gevolg dat lymfkliermetastasen hierachter verborgen

kunnen blijven of overschaduwd kunnen worden.

Met de introductie van TYR, kwam een tracer beschikbaar waarmee de eiwitsynthese in onder andere tumorweefsel is af te beelden. De sensitiviteit (83%) en specificiteit (95%) voor PET-TYR waren beter dan de resultaten van CT en MRI. Vergeleken met de PET-FDG resultaten had PET-TYR een betere specificiteit, accuratesse en positief voorspellende waarde. Daarentegen had PET-TYR meer vals negatieve resultaten dan PET-FDG. Een ander nadeel van TYR bleek de opname in de speekselklieren en in het beenmerg. Vooral de opname in speekselklieren gaf problemen met detecteren van lymfkliermetastasen die hier dichtbij waren gelegen.

De in hoofdstuk 3 en 4 gepresenteerde studies werd gebruikgemaakt van transmissiescans. Deze transmissiescans zijn nodig om de achtergrond verzwakking te meten. Hierdoor is de onderzoekstijd relatief lang (1,5 uur). In dit onderzoek werd nagegaan of het weglaten van de transmissiescan en daardoor verkorting van de onderzoekstijd negatieve gevolgen had. In hoofdstuk 5 worden hiervan de resultaten weergegeven. Het blijkt dat met behulp van het verkorte protocol (TYRWB) mogelijk is om vrijwel identieke resultaten te boeken als met de uitgebreide onderzoeksmethode.

In hoofdstuk 6 wordt de toepassing van PET beschreven bij het vaststellen van de mate van dysplasie en de detectie van chemisch geïnduceerde planocellulaire carcinomen op het palatum-slijmvlies van ratten. De mate van dysplasie werd gescoord met behulp van de Epithelial Atypia Index (EAI). Met PET-FDG kon geen correlatie worden aangetoond met de EAI. Dit was te verklaren doordat FDG ook wordt opgenomen in reactieve weefsels die bij het induceren van dysplasie in het palatum ontstaan. TYR daarentegen toonde wel een correlatie met de EAI.

In deze studie werd tevens een correlatie aangetoond tussen TYR en de dikte van het epitheel. Het lijkt erop dat de hyperplasie van het epitheel bepalender is dan de andere kenmerken van dysplasie voor de opname van TYR in dit model.

Voor het klinische gebruik van PET is het belangrijk om te weten wanneer een verhoogde opname van TYR correspondeert met ernstige dysplasie. Op basis van de beschikbare gegevens is het mogelijk om hierop te kunnen discrimineren. Of deze gegevens uit proefdieronderzoek ook kunnen worden gebruikt bij de mens zal moeten worden onderzocht.

In hoofdstuk 7 werd de mogelijkheid onderzocht om onbekende primaire tumoren met behulp van PET-FDG op te sporen. Gezien de goede sensitiviteit bij het opsporen van metastasen van planocellulaire carcinomen in het hoofd-halsgebied en de halfwaardetijd, die WB-scanning toelaat, leek FDG de meest geschikte tracer. In 30% van de patiënten met een metastase van een onbekende primaire tumor bleek het mogelijk deze met PET-FDGWB op te sporen. Het gebruik van PET is wel gelimiteerd door de resolutie van de camera. In de praktijk blijkt dat

primaire tumoren kleiner dan 6 mm zijn niet op te sporen. De waarde van TYR voor dit onderzoek dient nog onderzocht te worden.

### Algemene beschouwing

Positron Emissie Tomografie is een nieuwe benadering in de kankerdiagnostiek. In tegenstelling tot CT, MRI en US, worden biochemische processen in de patient afgebeeld. Met behulp van de tracer FDG wordt, de glucose consumptie van weefsels kunnen worden onderzocht. De tracer TYR geeft inzicht in de eiwitsynthese van tumoren en metastasen. Desalniettemin heeft PET ook beperkingen, deze worden gedeeltelijk veroorzaakt door de gebruikte tracer en gedeeltelijk door de apparatuur.

Voor PET onderzoek is niet alleen een camera vereist, tevens dient men de beschikking te hebben over een cyclotron en een radiochemisch laboratorium om kort levende radioactieve tracers te produceren. Dit maakt PET een relatief dure onderzoeksmethode en vraagt om goede logistieke procedures. Over kosteneffectiviteit is moeilijk iets te zeggen. De kracht van de methode in de hoofd-hals oncologie is vooral dat cervicale metastasen tussen de 5 en 10 mm gedetecteerd kunnen worden. Alleen USgFNAC is in prijs goedkoper, maar het is een invasief onderzoek dat erg onderzoeker-afhankelijk is. In vergelijking met de nu algemeen beschikbare diagnostische methodes die aanvankelijk in de experimentele fase ook erg duur waren, mag verwacht worden dat PET-diagnostiek in de toekomst goedkoper zal worden.

De resolutie van de camera is een belangrijke beperkende factor bij PET onderzoek. In de verschillende onderzoeken in dit proefschrift wordt als minimale grote van gedetecteerde metastasen 4 tot 6 mm aangegeven. In één geval was er zelfs sprake van een plasmocytoom van 3 mm. Op basis van de resolutie van de camera zal een metastase groter moeten zijn dan 5 mm voor een betrouwbare detectie.

De gebruikte tracers tonen een hoge sensitiviteit maar de specificiteit wordt beïnvloed door verschillende factoren. FDG toonde veel vals positieve reactieve lymfklieren terwijl de opname van TYR in de speekselklieren storend kan werken op de detectie van lymfkliermetastasen.

Indien PET wordt gecombineerd met een transmissiescan duurt het onderzoek ongeveer 1,5 uur en is mede daardoor onaangenaam voor de patient. Dit resulteert tevens in een minder efficiënt gebruik van de apparatuur. Het reduceren van de cameratijd door de transmissie scan achterwege te laten gaf resultaten die vergelijkbaar waren met onderzoeken waarbij wel een transmissiescan werd gemaakt.

Het detecteren van premaligne aandoeningen in een proefdiermodel is met behulp van PET-FDG niet mogelijk. Met PET-TYR daarentegen werd wel een relatie tussen dysplasie en de opnameactiviteit van TYR gevonden.

In het onderzoek naar onbekende primaire tumoren met metastasen in de hals draagt PET-FDG in 30% bij tot een betere detectie, waardoor een gerichtere



behandeling mogelijk is.

De onderzoeken gepresenteerd in dit proefschrift tonen aan dat PET in de volgende situaties in de hoofd-halsoncologie gebruikt kan worden:

1. In geval van een planocellulair carcinoom uitgaande van het slijmvlies van de bovenste adem- en voedingsweg kan met behulp van PET-FDG een negatieve hals worden bevestigd. Vanwege de hoge sensitiviteit en negatief voorspellende waarde van PET-FDG kunnen lymfkliermetastasen, groter dan 5 mm met een grote zekerheid worden uitgesloten.
2. In geval van een planocellulair carcinoom uitgaande van het slijmvlies van de bovenste adem- en voedingsweg kunnen met behulp van PET-TYR halskliermetastasen worden aangetoond. Vanwege de hoge specificiteit, accuratesse en voorspellende waarden van PET-TYR zijn metastasen, groter dan 5 mm met een grote zekerheid aan te tonen.
3. Om met behulp van PET-FDG in "wholebody mode" onbekende primaire tumoren te detecteren van halskliermetastasen.

## Curriculum vitae

De auteur werd op 20 november 1965 geboren in Enschedé. Na eerst de havo te hebben doorlopen werd in 1985 met goed gevolg het examen Atheneum B aan het Sint Maartenscollege in Groningen/Haren afgelegd. In februari 1991 slaagde hij voor het tandartsexamen aan de Rijksuniversiteit Groningen. In het tweede en derde jaar van zijn studietijd werd tevens de studie econometrie gevolgd. Vanwege de sluiting van de Faculteit werd prioriteit gegeven aan de opleiding Tandheelkunde en werd de studie econometrie niet voortgezet. Vanaf 1 april 1991 was hij vier dagen per week werkzaam als onderzoeker bij de afdeling Mondziekten, Kaakchirurgie en Bijzondere Tandheelkunde te Groningen. Gedurende 1 dag per week was hij werkzaam als tandarts in de tandartspraktijk drs. F.G.R. Chin a Paw te Hoogezand. Vanaf 1993 werd de tandheelkunde tevens beoefend in de praktijk van dr. H.P. de Jong en dr. W. Reuland te Roden. Per 1 november 1994 heeft hij de praktijk overgenomen van mevrouw Reuland. De aanstelling als onderzoeker op de afdeling Mondziekten, Kaakchirurgie en Bijzondere Tandheelkunde werd toen teruggebracht tot één dag per week.

## Dankwoord

Toen ik in 1991 afstudeerde had ik nog nooit over het doen van onderzoek nagedacht. Het meest moeilijke vak tijdens mijn studietijd was de oncologie, alhoewel het mij wel intrigeerde. In de onderzoekswereld ben ik tamelijk onverwacht verzeild geraakt. Toen ik belangstelling voor een onderzoeksplaats had getoond had ik voor dat ik het wist een sollicitatiegesprek bij prof. dr. G. Boering, toentertijd hoofd van de afdeling. Zoals iedereen die een proefschrift heeft geschreven weet, komt zoiets niet vanzelf tot stand. De waarde van de hulp van al degenen die een bijdrage hebben geleverd aan dit proefschrift moet niet worden onderschat. Dit geldt ook voor degenen die interesse hebben getoond of waarmee je even een goed gesprek kon hebben. Een aantal personen wil ik met name noemen.

Professor Roodenburg; beste Jan. Jouw inzicht en vermogen om duidelijk uiteen te zetten waar de essentie ligt bij het verrichten van onderzoek, hebben voor een belangrijk deel bijgedragen aan de totstandkoming van dit proefschrift. Tevens heb je door het opzetten van MON-4 een groep mensen om je heen verzameld waar menig hoogleraar jaloers op kan zijn.

Professor Vaalburg; geachte professor. Uw voortdurende belangstelling en de tijd die u heeft vrijgemaakt om manuscripten met mij door te spreken heb ik als zeer positief ervaren. Daarnaast heeft u een afdeling gecreëerd waar het verrichten van onderzoek zeer goed mogelijk is.

Professor Vermey, geachte professor. De wijze waarop u manuscripten corrigeert is ongeëvenaard. De nauwkeurigheid en accuratesse van uw correcties heeft het proefschrift erg veel goed gedaan. Hiervoor wil ik u hartelijk danken.

Dr. Nikkels, beste Peter. Vele uren hebben we tegenover elkaar gezeten. Ik bij jou en jij bij mij. Jouw histologische kennis was onontbeerlijk voor dit onderzoek. Gezien het feit dat je nu in Utrecht werkzaam bent maakt dat het contact wat verwaterd. Toch wil ik op een geschikt moment nog eens verder praten over de pathologie.

Dr. Pruijm, beste Jan. Jouw meedenken en meewerken aan dit onderzoek heb ik zeer gewaardeerd. Jouw bijdrage bestond niet alleen uit tekstuele zaken maar ook uit het inbrengen van vele infusen, arteriële lijnen en het beoordelen van de PET-plaatjes.

Professor Boering; geachte professor. Uw belangstelling naar de voortgang van het onderzoek ook na uw afscheid heeft mij zeer gestimuleerd.

Professor de Bont; geachte professor. Dat op de afdeling uitgebreid onderzoek kan worden verricht moet voornamelijk op uw conto worden geschreven. Er heerst een goed onderzoeksklimaat dat voor onderzoekers belangrijk is. Mijn hartelijke dank voor de gelegenheid om mijn onderzoek te kunnen voltooien.

Prof. Molenaar, Prof. Albers, dank voor het zitting nemen in de promotiecommissie van dit proefschrift en de zorgvuldige lezing van het manuscript. Prof. Reske thank you very much for your participation in judging this thesis.

Ik wil alle patienten bedanken die zich vrijwillig beschikbaar stelden om de vaak langdurige en vermoeiende PET-onderzoeken te ondergaan.

Philip Elsinga, Lizette Eriks, Moniek Hanko, Gert Luurtsema, Jitze Medema en Hilde Siertsema allemaal bedankt voor de FDG en Tyrosine. Mede door jullie inzet konden we onze experimenten doen. Anne-miek van Loenen natuurlijk hoor je ook in dit vorige rijtje thuis maar jij deed meer. Al die rattenstaarten met infuusjes kwamen uit jouw hand. Remy Schmeits, Johan Wiegers, Tonnie Wiegman en Marsha Zwartjes jullie bedienden de knoppen van de camera, zonder jullie gebeurde er niets.

Marjon Duim en Fieke Wiersema bedankt dat jullie elke keer maar weer de statussen voor me op wilden zoeken, en me waarschuwden wanneer er weer een aanvraag was ingediend. Gerda Boezerooy, Karin Wolthuis en Harry de Jonge bedankt voor de secretariële en administratieve ondersteuning.

Corina Nooren, altijd op de achtergrond maar altijd aanwezig. De stille kracht achter het 4NQO onderzoek. Je verdient een grote pluim.

Max Witjes en Ferry Woldring, geachte paranimfen. Beste Max, grote waardering heb ik voor je gekregen door de manier waarop jij onderzoek hebt verricht. Ik heb dan ook veel van je kunnen leren in ons gezamenlijke onderzoek. Beste Ferry, vele uren hebben we naast elkaar gestreden helaas de laatste keren met wat minder succes.

Alle overige medewerkers van de afdeling Mondziekten Kaakchirurgie en Bijzondere Tandheelkunde, wil ik bedanken voor de collegiale samenwerking.

Jan en Joke, bedankt voor alles wat jullie me hebben gegeven en voor jullie grote, nimmer aflatende belangstelling voor alles wat ons bezig houdt.

Annet, zonder jouw onvoorwaardelijke steun was ik nooit zover gekomen. Jouw energie om elke keer maar weer het huis gezellig te maken als ik er weer een troep van maakte is bewonderingswaardig. De laatste maanden waren hectisch maar we hebben ons erdoor geslagen. Ik hou van je.